IEEE Access
Multidisciplinary | Rapid Review | Open Access Journal

Received June 29, 2019, accepted July 16, 2019, date of publication July 19, 2019, date of current version August 8, 2019.

Digital Object Identifier 10.1109/ACCESS.2019.2930111

A State-of-the-Art Survey for Microorganism Image Segmentation Methods and Future Potential

FRANK KULWA[1], CHEN LI[1], XIN ZHAO[2], BENCHENG CAI[2], NING XU[3], SHOULIANG QI[1], SHUO CHEN[1], AND YUEYANG TENG[1]

[1]Microscopic Image and Medical Image Analysis Group, MBIE College, Northeastern University, Shenyang 110169, China
[2]Environmental Engineering Institute, Northeastern University, Shenyang 110169, China
[3]School of Art and Design, Liaoning Shihua University, Fushun 113001, China

Corresponding author: Chen Li (lichen@bmie.neu.edu.cn)

This work was supported in part by the National Natural Science Foundation of China under Grant 61806047, in part by the Fundamental Research Funds for the Central Universities under Grant N171903004, Grant N171902001, and Grant N180719020, in part by the Scientific Research Launched Fund of Liaoning Shihua University under Grant 2017XJJ-061, and in part by the China Scholarship Council under Grant 2017GXZ026396.

ABSTRACT Microorganisms play a great role in ecosystem, wastewater treatment, monitoring of environmental changes, and decomposition of waste materials. However, some of them are harmful to humans and animals such as tuberculosis bacteria and plasmodium. In such course, it is important to identify, track, analyze, consider the beneficial side and get rid of the negative effects of microorganisms using fast, accurate, and reliable methods. In recent decades, image analysis techniques have been used to address the drawbacks of manual traditional approaches in the identification and analysis of microorganisms. As image segmentation being an important step (technique) in the detection, tracking, monitoring, feature extraction, modeling, and analysis of microorganisms, different methods have been deployed, from classical approaches to current deep neural networks upon different challenges on microorganism images. This survey comprehensively analyses the various studies focused on developing microorganism image segmentation methods in the last 30 years (since 1989). In this survey, segmentation methods are categorized into classical and machine learning methods. Furthermore, these methods are subcategorized into threshold-based, region-based, and edge-based which belong to classical methods, supervised and unsupervised machine leaning-based methods which belong to machine learning category. A growth trend of different methods and most frequently used methods in each category are meticulously analyzed. A clear explanation of the suitability of these methods for different segmentation challenges encountered on microscopic microorganism images is also enlightened.

INDEX TERMS Microorganism segmentation, content-based microscopic image analysis, feature extraction, microscopic images, classical methods, machine learning.

I. INTRODUCTION

There are varieties of tiny microoganisms which play a great role in humans and plants lives, for balancing the ecosystem, food processing, water cleaning processes and promoting growth of plants [1]. Some are also harmful to human health, environments and other living organisms. In this review, recent microorganism image segmentation techniques are introduced. It is noted that there exist some review works on image segmentation techniques, for example, [2]–[4] and [5]. However, these reviews are based on segmentation of non-microorganism images except only in our previous review in [5], which gives overview on microorganism image analysis (partially, including segmentation). Furthermore, no concrete conclusions are pinpointed on the best segmentation methods for particular microorganism segmentation challenges or most frequently used ones. Thus, we attempt to fill this interesting research blank by a review of around 85 works.

The associate editor coordinating the review of this manuscript and approving it for publication was Habib Ullah.

A. MOTIVATION ON AUTOMATIC IMAGE SEGMENTATION OF MICROORGANISMS

Microorganisms are very small living organisms which can appear as unicellular, multicellular and acellular types [6]. Some are beneficial and some are harmful to human health and environments. For example, Lactobacteria are beneficial microorganisms, which decompose substances to give nutrients to plants [7]. *Mmicrothrix parvicella* which cause bulking in activated sludge [8], plasmodium and microbacteria tuberculosis which cause malaria and tuberculosis, respectively are harmful microorganims.

Good insight into microorgnisms helps in taking advantage of their beneficial side and reduce (eradicate) the negative effects of harmful ones. It is so rare to find microorganisms in isolated environments. Microorganisms are found almost everywhere, in unclean fluids, air, soil and as parasites in other organisms. Most of them have features (for example color and size) which cannot be easily distinguished from their settling environments by naked eyes. Thus manual and (or) automatic processes are required to isolate them. Some of the manual processes involve culturing and staining some samples which are rich in microorganisms [9] and use of magnification tools such as microscope for viewing. After viewing, analysis can be done manually (traditionally) using experts, or automatically using image segmentation and other image processing techniques.

Automatic image segmentation plays the following roles in image analysis:

- Feature extraction: Segmentation is usually an important step before feature extraction, as it partitions and isolates the foreground from other parts of the image. Then features like shape, color and texture of the foreground can be extracted easily. For example, [10] used adaptive color based thresholding and edge detection method to segment tuberculosis microbes, then extracts shape featured (area, major axis length, minor axis length and perimeter).
- Tracking: Image segmentation is very useful when tracking microorganisms in videos which are captured under microscope. Tracking helps to get insight into the mobility, genetic and quantitative characteristics which are needed for research works [11].
- Modeling and Analysis: Segmentation is very applicable in modeling and analysis of microorganisms. The results of modeling are used in studying microorganisms development, genetics and their corresponding neurobiology. For example, [11] used Neyman Peason decision approach to segment *C. elegans* for modeling and tracking video images of micro-worms.
- Detection: Identification of the desired microorganisms on an image can be done directly after segmentation [12].
- Monitoring: It is the process of observing the progress of microorganism over a period of time. Image segmentation is useful in monitoring characteristic changes of the microorganism. For example, [13] used Otsu thresholding method for automatic monitoring of floc and filaments in activated sludge water treatments process.

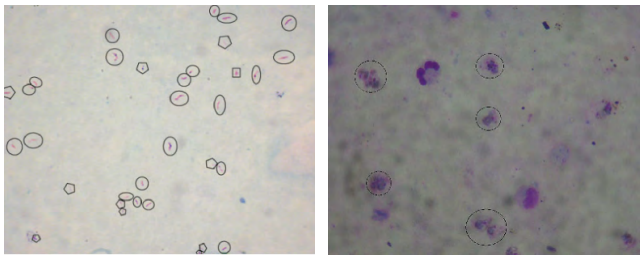

(a) (b)

FIGURE 1. Manual segmentation to indicate the presence of parasites on microscopic images performed by biologists where, (a) TB bacteria manually segmented from sputum smears [31], (b) Encircled *plasmodium* (malaria) parasite from blood smears [32].

Given that image segmentation is of significant importance in various microorganisms tasks including monitoring, detection, tracking and modeling, different approaches for segmentation have been proposed. In this review these methods are grouped into classical and machine learning based methods as listed below:

Classical segmentation methods include [14]:

- Edge based segmentation methods (EBS), such as Canny edge detection [15], active contour model [16] and Marr Hildreth edge detection [17].
- Threshold based segmentation methods (TBS), such as Otsu thresholding [18].
- Region based segmentation (RBS), such as watershed [19].

Machine learning based methods, consist of the following:

- Supervised machine learning methods (SML), such as support vector machine [20], [21] and convolution neural networks like U-net and VGG-16 [22], [23].
- Unsupervised machine learning methods (USML), such as fuzzy c-means clustering [24], k-means clustering [25] and generative adversarial networks (GANs) based techniques [26]–[28].

B. TRADITIONAL MICROORGANISM SEGMENTATION METHODS

Traditionally, manual approaches are used for segmentation (identification) of microorganisms. The most common way is the application of morphological methods to identify microorganisms after observation under microscopes, which is done manually by biologists (experts), using some image processing softwares [29], [30]. Fig. 1 illustrates manual way of segmenting microorganism from microscopic images of TB bacteria and *Plasmodium*.

Although traditional methods are advantageous, like being real time and flexible to changes of examined samples characteristics, they are subjected to the following drawbacks: Time consuming, tedious work, biased to experts skills, inconsistent, expensive and the results may be affected by experts

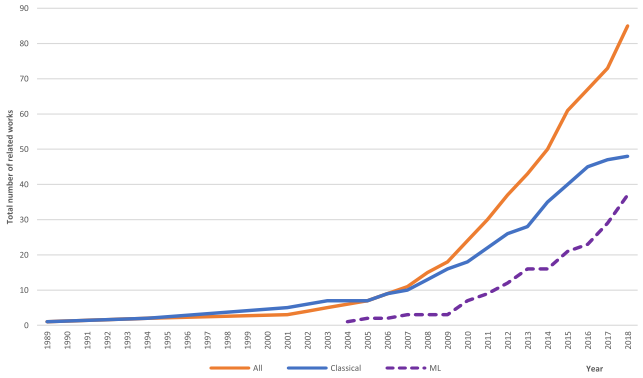

FIGURE 2. Development trend on microorganim image segmentation methods. Indicating, machine learning (ML) based methods, classical methods and general trend (All).

daily moods. These drawbacks prompt the need for alternative, suitable and reliable methods.

C. AUTOMATIC MICROSCOPIC MICROORGANISM IMAGE SEGMENTATION METHODS

Segmentation is a process of partitioning image into some non-intersecting regions such that each region is homogeneous and the union of two adjacent regions is heterogeneous [2]. Traditional approaches for segmentation are over-weighed by their drawbacks like time consuming and inconsistency. To get rid of such drawbacks, the application of automatic segmentation methods come to hand. Automatic image segmentation means, no involvement of human in the processes of partitioning and identification of the desired part on an image unless in the algorithm design process. Computer algorithms are used to partition images into segments so that analysis can be done. Contrary to traditional approaches, automatic image segmentation is faster, consistent, accurate and generally cheap. For example, in medical field, automatic image segmentation helps in fast, reliable and consistent diagnosis of diseases, identification and classification of pathogen, which contributes to saving lives [33]. Due to its advantages, so many recent researches are performed on segmentation of different microorganism images. The development trend over recent decades is shown in Fig. 2.

Owing to the role of microorganisms in our life circle and many researches being focused on automatic image segmentation, we attempt to write this review paper aiming at pinning out the most frequently used methods and their technical advantages to specific microorganism image segmentation challenges. For a grasp on categories of image segmentation methods as described in this review, Fig. 3 shows important steps in automatic image segmentation pipeline, which include data acquisition, color conversion, image enhancement, denoising, image segmentation techniques and their respective categories and subcategories.

From the flow chart in Fig. 3 we can find that:
Stage (1): Is acquisition of microorganism images which is normally done from samples under microscope. Microorganisms can be from agricultural field, food processing field, medical or other fields. Most common classes of microorganisms of interest are bacteria, archaea, protists, animals, fungi, plants and virus [34].

Stage (2): Image conversions and enhancement take place depending on visual and contrast characteristic of microorganism against background on image. Common conversions are RGB to gray scale, RGB to HSV, RGB to LAB, RGB to HSI and RGB to CMYk color modes. Denoising is also done at this stage using one of the existing filters like Gaussian filter, mean, median filters and other possible denoising techniques depending on the nature of noise on an image.

Stage (3): Is the segmentation phase, in which microorganisms are isolated from background and other artifacts. Suitable methods sorted between two categories (a) or (b), classical or machine learning methods can be applied for segmentation. Classical methods include subcategories ((a)i-iii) which are threshold based, like Otsu (which segments images on the bases of intensity values to get a binary image), region based and edge based methods like Sobel and Canny techniques. Threshold and edge based methods are normally applied to gray scale images.

The most common supervised learning methods ((b)(i)) are convolution neural networks, support vector machine and naïve Bayes classifiers. Neural networks do not need much preprocessing like RGB to gray conversion as they are capable of working directly on the coloured images, also they do not need pre-defined features to enable segmentation contrary to SVM which needs pre defined features. The most common unsupervised methods for segmentation ((b)(ii)) are similarity based clustering methods like fuzzy and k-means related ones.

D. STRUCTURE OF THIS REVIEW

In this article, a broad overview of microorganism image segmentation is presented with interconnected pipelines. Firstly, it surveys related researches by their segmentation methods (category and subcategory). Secondly, it surveys these works by their time line since 1989 to 2018. Time line helps the reader to get a big picture on the development trend of related segmentation techniques, in conjunction to innovation of new and better ways of solving image segmentation challenges in microorganims. For instance, from linear classifiers such as SVM to nonlinear classifiers such as convolution neural networks, from convolution neural networks which classify images into image wise labels such as VGG-16 [35], to pixel wise classifiers such as SegNet [36], U-net [23] and FCN [22]. Current methods can be built on top of previous methods for improvement or innovated as new approaches. For example, the encoder parts of SegNet and U-net are built on top of VGG-16 which is seen as a novel method [37]. Furthermore, in this review, research motivation, contribution, methodology and segmentation results are briefly summarized for each reference. For some related works with important methods and results, demonstration figures are shown for clarifications. Table. 3, in appendix V, gives a general

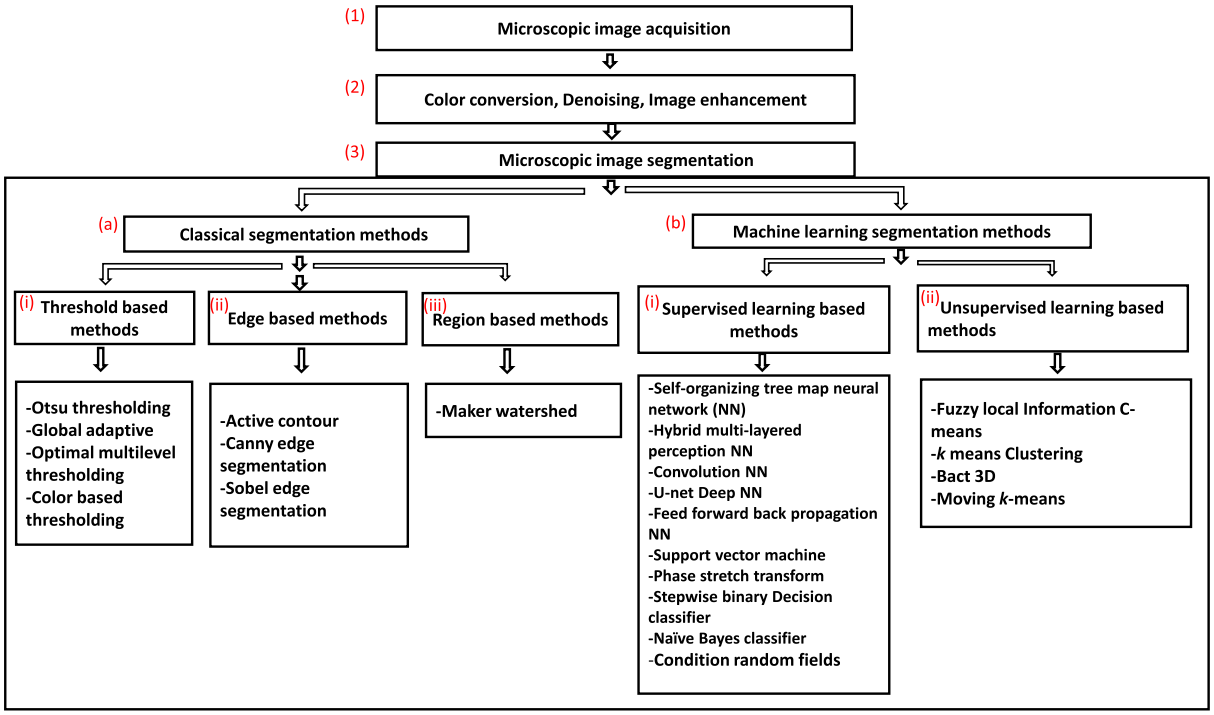

FIGURE 3. General pipeline for automatic image segmentation of microorganisms, (1) image acquisition, (2) image enhancement and denosing, (3) segmentation.

overview of two pipelines (applied methods in chronological order) of the surveyed works.

This review is structured as follows, Sec. II reviews classical segmentation methods and a brief analysis is given at the end of this section on the advantages of the most frequently used methods. Sec. III gives a comprehensive review on machine learning based methods for segmentation, and brief analysis is also included at the end of this section. As a subset of USML, a brief overview of GANs is given at the end of Sec. III-B and in Sec.IV-D. Then a profound methodology analysis on suitable segmentation techniques for specific images segmentation challenges and most frequently used methods are discussed in Sec. IV. Finally a brief conclusion is given in Sec. V. This review can illuminate related researchers on most applicable, suitable and recent segmentation methods of microorganism images.

II. CLASSICAL METHODS FOR SEGMENTATION OF MICROORGANISMS

Classical image segmentation methods include threshold, edge and region based segmentation techniques. Threshold techniques are the simplest methods in which segmentation is based on the selection of threshold values to convert a gray scale image into a binary image [38], examples are Otsu, iterative thresholding, global thresholding, local thresholding and multithresholding. Edge based techniques transform image to edge binary image benefiting from abrupt changes in gray tones in the image [39], examples are Canny, Sobel and active contour. Region based techniques divide the entire image into sub-regions, examples are maker watershed, H-minima transform and concavity. Owing to the fact that some techniques are suitable for segmentation of particular images [2], an overview of classical methods related works as applied to microorganism image segmentation is given in subsections below.

A. THRESHOLD BASED SEGMENTATION (TBS)

For accurate segmentation of biofilm clusters which are characterized by unclear marking boundaries, [40] compares entropy and histogram based techniques, which are; Local entropy which uses spatial correlation in the image as criteria for selecting optimal threshold, joint entropy, relative entropy, Renyi's entropy, and iterative entropy (which is based on histogram and assumes the optimal threshold by averaging the mean value for both background and foreground pixels thus, it is suitable for poor contrast images). In the experiment, 660 × 480 pixel size, 8 bit (256 gray level) images of biofilms are used. With reference to manually segmented images as ground truth, the iterative selection method outperforms other methods by regression coefficient of 96.00%

Since segmentation is required prior to volume and interface area measurement of biofilm, in 3D image analysis from confocal laser scanning microscope (CLSM) [41], an objective threshold selection (OTS) technique, for selection of optimal threshold value is proposed in [41]. The optimal threshold value is found by finding the median of individual values on perpendicular plane of the 3D biofilm (derived from

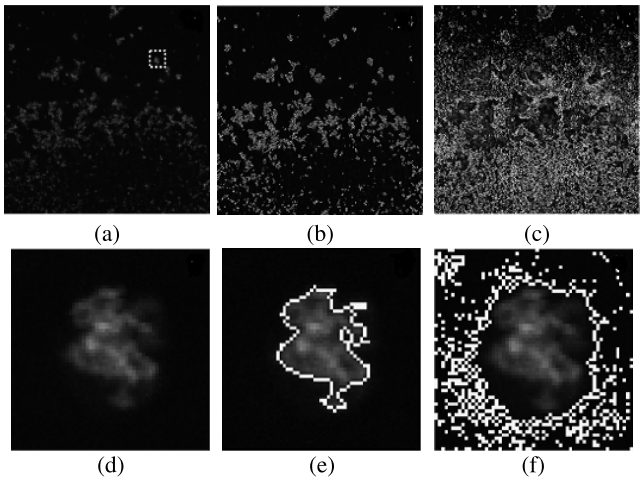

FIGURE 4. (a, d) Original CLSM images of staphylococcus aureus. (d, e, f) illustrate enlarged views of the regions encased by a dashed square in (a). (b, e) the segmented images using the 3D Otsu method and (c, f) the segmented images computed by OTS [43].

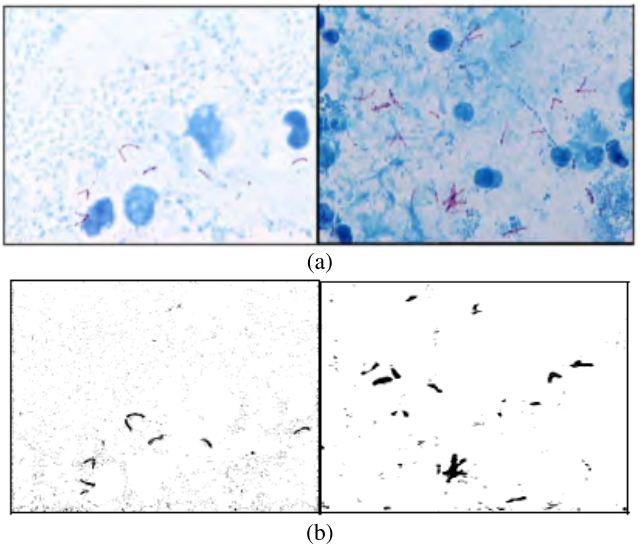

FIGURE 5. (a) Original colored images of TB bacteria, (b) threshold segmented images [46].

robust automatic threshold selection (RATS) method [42]). During experiments, biofilms from two kinds of culturing media are used (denitrifying and phenanthrene) and the segmentation results achieved are near to manual results. A related work is presented in [43], where, OTS approach is compared with 3D otsu based method on segmentation of CLSM biofilms images of *P.mirabilis* and *S.aureus*. In Otsu based approach, images of pixel size 1024×1024 are passed through anisotropic diffusion filter before performing 3D otsu segmentation. The results show that, Otsu based method in combination with filtering, gives better results than OTS. Fig. 4 shows the segmentation results of both methods on same dataset as presented in [43].

In segmentation of TB bacteria which are characterized by yellowish color in the fluorochrome auramine O stained sputum, color based segmentation which provides a broader discrimination between object borders is presented in [44]. The best channel for segmentation in RGB (which gives the optimal threshold value), is found to be blue by using Yager function for fuzziness. Then images are thresholded based on the value obtained in histogram of blue channel. Dilation and closing morphological operations are applied on segmented images, before shape features being extracted for classification. In this approach a set of 80 images from positive TB bacilli and 50 negative images are used for training and testing the classifier. This method achieves segmentation results with a specificity of 82.00%.

A segmentation technique for identification of *Mycobacterium tuberculosis* low contrast conventional light microscopic images of sputum is proposed in [45], where, subtracting green channel from red (R-G) is found to give a distinct visual identification of TB bacteria from the background, then binarization is performed using global adaptive thresholding for final segmentation. The algorithm is evalutated using 50 RGB images of size 3072×2304 pixels, obtained from positive TB sputum samples. Quite satisfactory segmentation results of 75.65% sensitivity are obtained by the proposed technique.

In [46], a color based approach for segmentation of TB bacteria from ZN stain sputum sample images is presented, where the RGB images are first divided into their corresponding R, G, B color channels, then threshold based segmentation is applied on each channel image separately. To get the segmented image the output of all channels are combined using AND operation (The pixel is defined as part of the foreground if its three RGB components all lie within the selected range). In the experiments, five images (of different types) are considered for initial studies and other 50 images for testing. The segmentation results are indicated in Fig. 5. This approach is compared with global thresholding method on the same dataset in [47], where, global thresholding is performed based on the C-Y color information of the image pixels which contains TB. The technique retains the red pixels of TB bacilli which fall in the range of hue 0^0 till 120^0 while the other pixels which fall in the range of 121^0 till 360^0 are eliminated. The results show that global thresholding produces better results compared to previous color thresholding, as it is able to reduce more noise and sputum background from the images. Fig. 6 shows the flow chart for comparison.

In [48], an edge linking based method to detect and separate individual *C. elegans* worms in culture is proposed. Gaussian smoothing with 20×20 pixels mask is applied, then subtraction of blurred image from original image is performed to keep the high frequency pixels (the edges). Then global thresholding is performed on the high frequency image. Finally, morphological skeletonization is performed followed by closing operations (to isolate and remove pixels and noisy branches). To detect individual worm in clumps, a skeleton analysis and tree reconstruction technique is applied on the binarized image. During experiments,

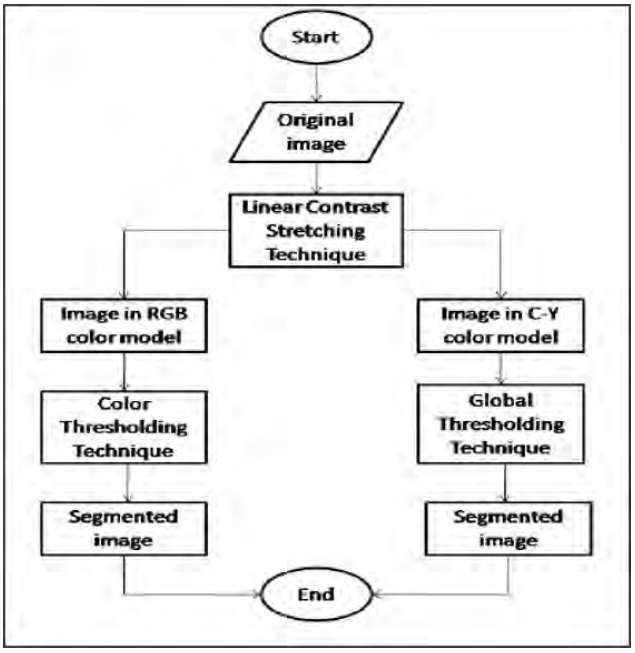

FIGURE 6. Global and color tresholding processes [47].

different combination of five population images that include 255 isolated overlapping *C. elegan* worms are used. Finally, an accuracy of around 83.00% is achieved on tested dataset.

HSV color mode offers a convenient representation of the color image than RGB, in [33], Hue channel is used to find optimal range occupied by bacilli by applying adaptive thresholding on stained images, in which bacilli appear reddish in color. Then shape descriptors are used for classification. In this work 300 (RGB images of 2045×1536 pixel size) taken from sputum smears of 3 patients are used and results are visually evaluated.

In order to automate fully the segmentation process while using multi-level methods, Otsu, entropy and minerror (which involve manual selection of threshold values), the combination of multi-level segmentation methods and method for determining the optimal threshold values are compared in [49]–[51]. Otsu, entropy and minerror segmentation methods are tested in combination with five methods for threshold values determination (Davies-Bouldin index (DB), Dunn's index (DN), Calinski-Harabasz's index (CH), Xie-Benil index (XB) and index I (I)). The best combination is found to be entropy and DB, since entropy is able to segment all kind of tested images (with single and multiple thresholds), while Otsu and minerror methods show poor segmentation results on single threshold images. In the experiments, 649 images of biofilm are used. These images are subset of two groups, 616 from confocal microscope (resolution of 512×512 pixels) and 33 images from an optical microscope with resolution of 1040×1392 pixels.

In [52], a digital segmentation and classification approach which is capable of identifying individual spiral bacterial cells from complex microbial community is presented, where

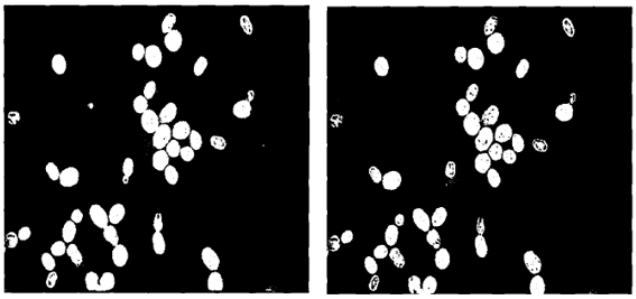

(a) Otsu method (b) Proposed method

FIGURE 7. Output results for Otsu only in (a) and for proposed method in (b) [53].

RGB to gray conversion is applied first, then binarization using global thresholding follows, then geometric features are found before classification using 3δ classifier, k-NN classifier, neural network classifier and fuzzy classifiers. In the experiments, 300 RGB images of Vibrio bacteria, 840 of Spirillium and 140 of Spirochete bacteria are used. Finally 3δ classifier yields an accuracy of 100%. k-NN yields 100% for $k = 5$. The neural network classifier 100% and fuzzy classifier 100% accuracy.

To eliminate contour background in optical microscopic images, a method is proposed in [53]. This approach reconstructs the background by calculating surface function minimizing least square error of the sampled image, then Otsu optimal thresholding elects pixels to be representative of the background and bilinear interpolation finds non deterministic background pixels among sample pixels, then 2D cubic fitting method is applied to construct a contour background. Elimination by subtracting approximated background from the original image is applied to achieve a segmented image. In the experiments, the dataset used are gray scale images of *Acinetobacter sp* and *Zygosaccharomyces rouxii* of size 640×480 pixels. The results of the proposed method are compared with results when applying Otsu's method only. Fig. 7 shows the segmentation results of the two methods.

In [54], as quantification of protein aggregation in *C. elegans* can be used for modeling protein aggregation in human for therapeutic strategies, a system for segmentation and quantification of protein aggregates in *C. elegans* 3D images is proposed. In this system 2D slices of the images are acquired, then anisotropic diffusion algorithm is applied for denoising, after this follows the global thresholding before morphological operations. Then 3D body reconstruction (using marching cubes algorithm to form cubic grids, followed by tri-linear interpolation between random points in the 2D image and all cubic grids) is performed. Finally quantification of several features on protein aggregates is done (such as volume and area). In the experiments, 150 images of *C. elegans* are used. The obtained results are consistent with quantitative observation in literature, allowing non biased reliable and high throughput protein aggregates quantification.

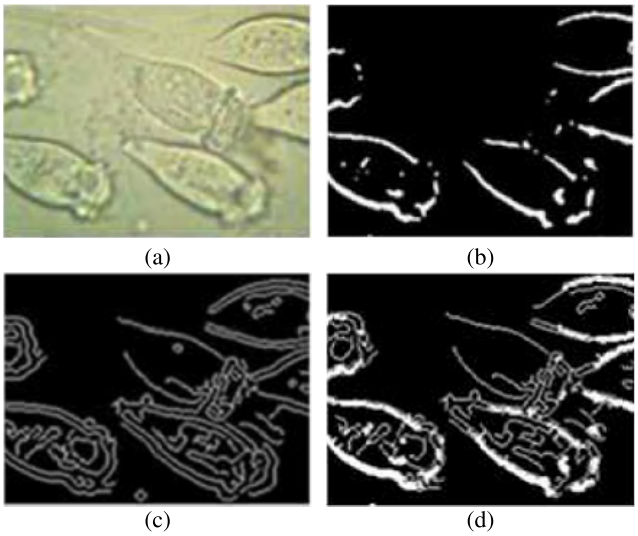

FIGURE 8. Segmentation results after iterative thresholding and canny edge detection. (a) Original epistylis image, (b) segmented image by Canny method, (c) segmented image by iterative thresholding, (d) image after fusing results in fig. (b) and fig. (c) based on wavelet [57].

[55] proposes an approach to segment hepatitis B virus from transmission electron microscopic (TEM) images. The method is based on binarizing the original image to identify the capsids. Since common segmentation or filtering techniques such as basic thresholding or unsharp masking are not suitable, because of the important size of the capsids, the poor contrast, SNR of TEM images, trous wavelets is used for segmentation due to its intrinsic multi-resolution properties, then follows skeletonization and graphical generation to circle the capsids. The tests is done on 9 image series, each series being composed of approximately 40 images of capsids (microscopic hepatitis B images). The ratio of the number of capsids detected by algorithm to that detected manually is used to evaluate the results. The mean ratio (accuracy) obtained is above 80.00% for all sets of tested data.

In order to segment TB bacilli from ZN trained tissue with uneven distribution of stain (dye), first global threshold is applied to remove tissue and background from blue dye [56], then k-means clustering segments bacilli from background, followed by mean filtering and adaptive thresholding for fine segmentation. 25 RGB images of positive TB stained tissues are used for testing the algorithm. And a segmentation accuracy of 99.00% is achieved.

In [57], a scheme to segment metazoa and protozoa from low contrast images of active sludge is proposed, where the image passes through two branches, first branch uses iterative thresholding which extracts the foreground from background and the second branch uses canny edge segmentation which enhances the foreground edges, then the two branches are fused together based on Mallat pyramid wavelet transform to get a fine segmented image. Microscopic gray scale images containing protozoa/metazoa are used during experiments. The results of each stage are shown in Fig. 8.

In order to segment floc and filaments from bright field microscopic images, which are characterized by images with comparatively less illumination near the boundaries, different algorithms based on Otsu thresholding are applied in [13]. These algorithms are named, local Otsu I, local Otsu II and local Otsu III. The best one is Otsu III and it is implemented as follows, First, Otsu global thresholding is applied, then bounding boxes are created for all detected objects and around the borders, then Otsu thresholding is applied again at all bounding boxes separately. Then all segmented boxes are rewritten to their pixel positions to get the whole segmented image. Different grayscale images of activated sludge of size 2088 $\times$ 1550 pixels are used, during experiments. The counts of flocs in proposed method are compared with manual counts and Otsu III achieves results near to manual counts.

In [58], due to the importance of green microalgae for giving signs to deterioration of ecological conditions, a segmentation algorithm of green microalgae images is proposed. In this approach, eigenvalues of the image are found first, then computation of multivariant Gaussian distribution parameters for algae and background is performed, before thresholding to get a binary image. During experiments, 44 RGB (600 $\times$ 800 pixel size) images of green algae taken from different species of selenestraceae family are used. The proposed method achieves an accuracy of 92.20%.

In [59], a thresholding program which is capable of segmenting irregularly illuminated images from activated sludge is present. Iterative region based Otsu thresholding is applied on bright field microscopic images of activated sludge (it is called iterative region based Otsu because it uses Otsu threshold technique recursively with a selection of foreground region at each iteration until suitable foreground is obtained). In the experiments, 40 RGB images (122 $\times$ 960 pixel size) captured from samples of activated sludge are used. The proposed method is compared with other Otsu based methods (iterative Otsu (IO), local adaptive Otsu (Loc-Otsu) and Otsu). The proposed method outperforms other methods with an accuracy of 98.50%.

To enhance diagnosis of malaria quickly, an accurate detection system of *Schizont plasmodium falciparum* from blood smear is introduced in [60]. First median filter is applied to remove salt and pepper noise, followed by color contrast enhancement on RGB images. Then RGB to HIS conversion is performed since a distinct threshold level between blood, parasite and background is easily observed in HIS mode, finally global thresholding is done. In the experiments, 100 RGB microscopic images (size 1600 $\times$ 1200 pixels) containing *Schizont plasmodium falciparum* are used. The segmentation results are evaluated visually as shown in Fig. 9.

Because shape similarity makes it difficult to identify protozoa, an identification system which uses 3D geometric multiple color channel local features is presented in [61], where segmentation is done by decomposing the image into color channels (RGB, R, G, B, gray scale, HSV, H, S, V

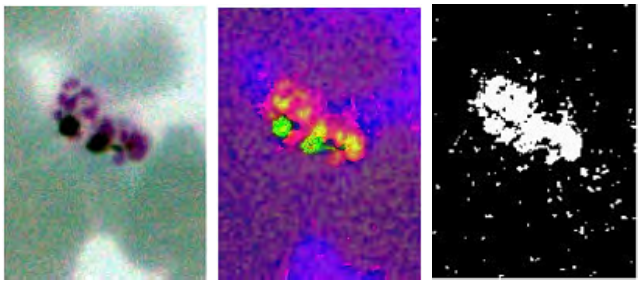

FIGURE 9. (a) RGB image, (b) HIS image, (c) final threshold segmented image [60].

and mean HSV (mHSV)), then for each color channel key points which are extracted by scale invariant feature transform (SIFT) are grouped. Then bag of visual words (BoVW) is used to calculate histogram of visual words as feature vectors. Finally classification is done using SVM to identify species of protozoa. 55 images containing 8 classes of protozoa, are used during experiments (classes are *Acantamoeba*, *Balantidium*, *Cystoisospora belli*, *Cyclospora cayetanensis*, *Iodamoeba butschilii*, *Giardia lamblia*, *Sarcocystis* and *Toxoplasma gondii)*. The proposed method achieves an accuracy of 96.00%.

B. REGION BASED SEGMENTATION (RBS)

In [62] an automatic segmentation system of bacteria microscopic images is developed, this system first segments the bacteria clusters from background using Otsu followed by region growing methods, secondly, seeds are selected at the center of individual bacteria in clusters, then seed watershed is applied to segment individual bacteria from clusters. This differs from the original watershed algorithm in that water is only pumped in at each seed location rather than at every local minima. RGB microscopic images containing *B. subtilis* bacteria are used during experiments.

In [63], segmentation and classification approach for rotavirus-A is proposed. Segmentation is performed on gray level images using marker controlled watershed method, which is able to identify closely spaced particles as individual objects in tested images. Then extracted shape features are used to train and test 3α classifier and min-max classifier. In this experiments, 50 RGB digital images containing rotavirus-A particles (non-overlapping) taken from transmission electron microscopy are used. Finally, 3α classifier method yields better results 98.00% classification rate.

A segmentation method for enhancing visualization and analysis of 3D laser scanning microscopic images of *C. elegan* cells is introduced in [64]. The approach involves five steps which are, acquisition, registration, segmentation using adaptive 3D watershed algorithm, reconstruction and analysis (quantification) of individual *C. elegan* cells based on their relative location patterns in the 3D standardized space. 3D input images of *C. elegan* taken from fluorescent laser scanning microscope are used for testing the algorithm. The final results are as shown in Fig. 10.

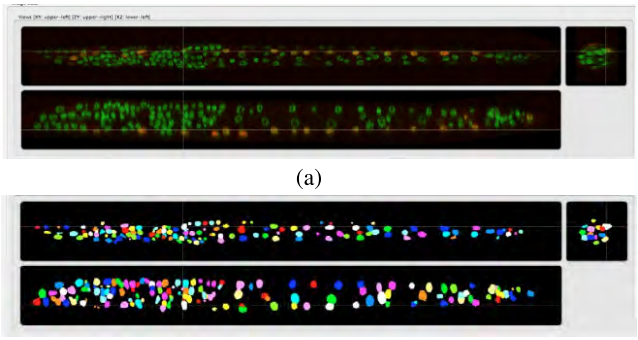

FIGURE 10. 3D image visualization and analysis for measuring single-cell gene expression of *C. elegans*, (a) tri-view display of a confocal image of *C. elegan* muscle cells, (b) tri-view display of the 3D watershed segmented nuclei of (a) [64].

A contour based seed region growing watershed technique is used to segment TB bacteria from their background in [65]. Before segmentation, color conversion to Lab color mode and denoising using image filling holes operations are applied. Then Hu moment and geometric features are used to further isolate the bacteria. During experiments, 516 RGB images with size 2080 × 1542 pixels are used for segmentation.

In [66], based on illumination conditions, different background colors, weak edge and low contrast which hinder better results in identification of bacteria in microscopic images of ZN stained sputum smear, an approach is proposed. Firstly, the Gaussian weighted adaptive threshold segmentation and local minimum points search within gradient image are applied to obtain the required markers. Then the marker-based watershed transform is employed for initial segmentation. Finally, multi-thresholding is applied for fine segmentation. In the experiment, 50 RGB images of positive TB are used. A segmentation accuracy of 83.8% is achieved.

For segmentation and motility modeling of C. elegans in [67], a single annotated image is used to compute a number of image texture features within a Bayesian model to infer which pixels belong to the nematode and which ones do not, then the mean-field variational inference technique is applied to compute the maximum posterior marginals of the pixel labels. Finally, Bayesian filtering, provides coherent estimates to where the nematode is located across the image sequence. 35 images each from different motility environments for *C. elegans* are used (crawling on an agar surface, swimming in an aqueous drop, swimming in gelatin based solutions, navigating through mazes constructed of micropillars, movement of nematode in aqueous buffer solution containing monodisperse particles and movement of nematode in aqueous buffer solution containing polydisperse particles). The proposed approach shows improved results compared to previous traditional intensity based thresholding and multi-environment model estimation (MEME) algorithms.

In [68], a system to monitor morphological features of floc and filaments in activated sludge which uses segmentation approach is introduced. It uses H-minima transform (region based method), followed by median filter, finally

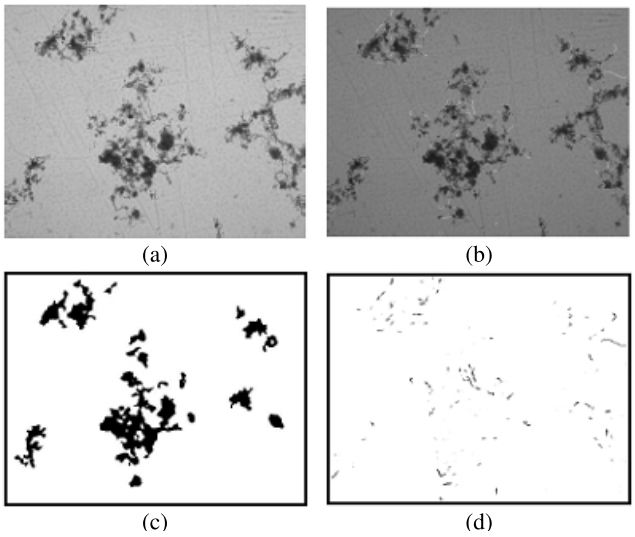

FIGURE 11. (a) Original gray scale image, (b) superimposed filament segmentations, (c) floc segmentation, (d) filament segmentation [68].

conventional binary conversion and area opening operation are applied. 30 grey scale images captured under the bright field microscope from activated sludge samples are used in the experiments. Fig. 11 shows the flow of image from original to segmented one.

In order to separate overlapping bacilli a method of concavity (MOC) is used in [69], where concavities are found using the convex hull of the segmented binary image. Fig. 12 shows the MOC algorithm. 100 images of size 4164 × 3120 pixels containing overlapping bacilli are used during experiments. Finally, the individual counts of TB bacteria is obtained after segmentation. MOC results are compared with manual results, and other conventional methods (multi-phase active contour and marker controlled watershed). The results of MOC are more similar to manual (ground truth).

In [70], a detection algorithm is proposed to segment and classify TB bacilli from microscopic images captured by smart phone camera. In the algorithm, RGB to gray level conversion takes place, followed by contrast enhancement, then thresholding and morphological operations are applied, after this, the artefacts are removed based on shape and size (to remain with bacilli only), then watershed method is applied for separation of overlapping (touching) bacilli, finally counting and labelling of bacilli is done. In evaluation of the proposed method, 30 RBG images of ZN stained bacilli taken from smart phone camera enabled microscope are used. 15 images are TB positive and 15 are TB negative. The overall segmentation result of the proposed method is 87.00% specificity.

C. EDGE BASED SEGMENTATION (EBS)

In [71], a segmentation and classification framework is introduced to identify individual microorganism from a group of overlapping (touching) bacteria. Canny edge segmentation is applied prior to Yanowitz bruckstein which are found to give better segmentation results on such images containing non

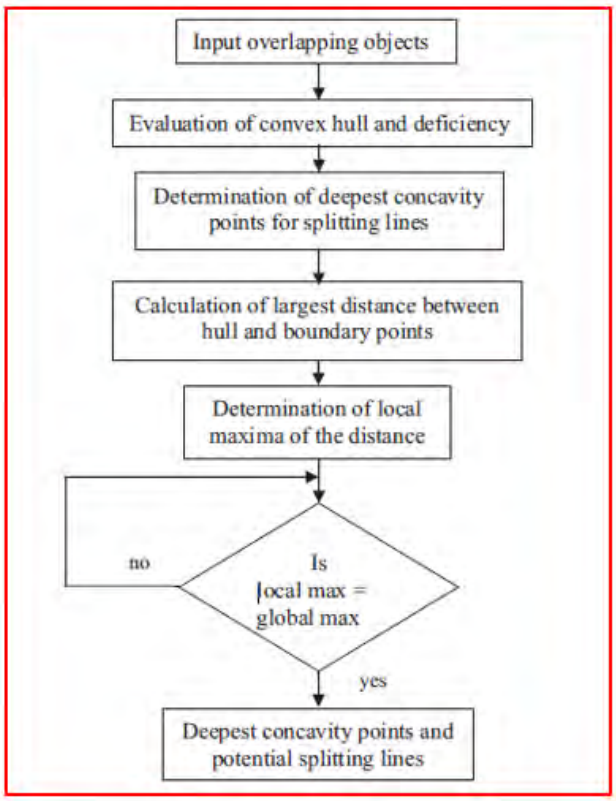

FIGURE 12. Flow chart for method of concavity [69].

uniform illuminating backgrounds, then shape coefficient and eigenvalue ratios are used as features for classifying between individual microorganisms and in which particular group they belong. In the experimental analysis, contrasts photomicrographs of growing culture were used as inputs images and two *Methanogenic* bacteria are used as model organisms (*Methanosprillum hungatei* and *Methanonosarcina mazei*). Two categories of images are used, one category is the image set containing only one specie of microorganism. Another is the one containing mixture of two species. Finally, the result is given in counts of bacteria in tested images. And it shows that the count is very near to accurate manual count. Fig. 13 shows the segmentation work flow.

In [72], evaluation of suitable segmentation (technique which is capable of segmenting bacteria and protista biomass so as to understand their population parameters) is presented. The following thresholding techniques are evaluated: Visual (VIS), middle gray level (MID), maximum first derivative (MAXD1), minimum of histogram of high-gradient pixels (MINASH), maximum of the histogram of high-gradient pixels (MAXASH), average of the histogram of high-gradient pixels (AVGASH), minimum of the quotient of histogram and gradient (MINSH/D1), maximum of the product of histogram and gradient (MAXSH*D1), minimum of the second derivative (MIND2). In the experiments, 144 RGB images of microspheres which are taken under fluorescent light are used. The size of spheres in image are 0.51, 0.94, 3.1 and 6.1μ. Also 50 to 60 images of cells from the following cultures

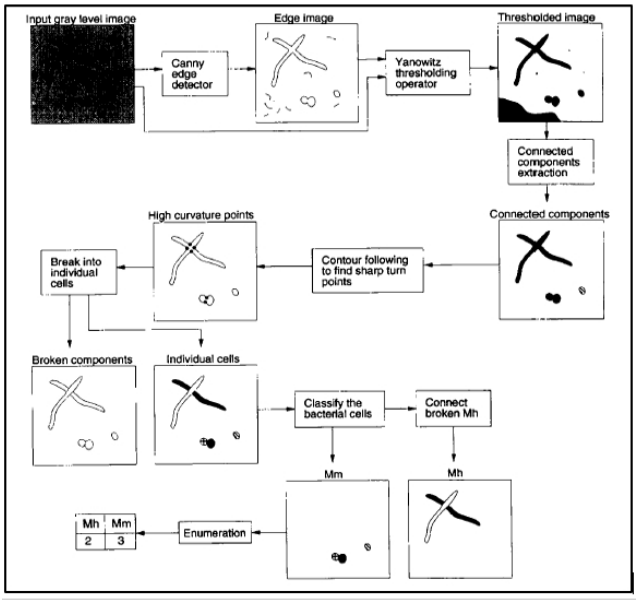

FIGURE 13. Flowchart for segmentation and classification of bacteria in mixed culture. Mm = *Mathanosarcina maise* and Mh = *Methanospirillium hungatei* [71].

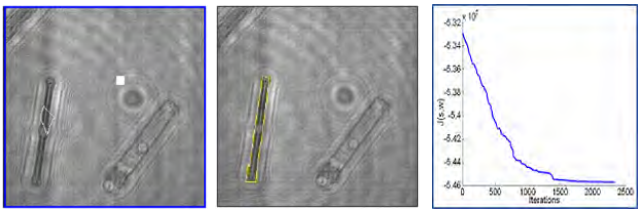

FIGURE 14. (a) Snake evolution on a diatom algae with four point contour initialization, (b) final segmentation with bivariate region snake after 1500 iterations, (c) optimization trace during experiment [74].

are used, cyanobacterua, cryptophyte, marine phytoplankton, flagellate and ciliates. Comparing all the tested approaches, the best one is minimum of the second derivative (MIND2) which achieves the average lowest segmentation errors.

An automatic identification of tuberculosis bacteria (from fluorescent microscopic images of stained samples with fluorochrome auramine O) is proposed in [73]. Since bacteria appears brighter yellowish on tested images, Canny edge technique is applied for edge detection, followed by a non-maxima suppression and a hysteresis threshold operations. Because some structures can appear broken, a morphological closing operation is applied. Then compactness and eccentricity features are extracted in one branch, and the same segmented images are passed through k-means clustering in the second branch, then each branch independently goes to classification part using nearest neighbor classifier. A total of 397 negative and 75 positive RGB images are used. The average results obtained from two branches are, 93.30% and 100% sensitivity for the first and the second branch, respectively.

To be able to segment 3D holograhic images of microorganism, an approach is proposed in [74], which uses statistical region snake (active contour model) method which is performed in many number of iterations to have better segmentation results. 3D digitally constructed images of sphacelaria algae and diatom algae are used for experiment. The obtained result is shown in Fig. 14.

In [75], a system capable of identifying individual rod like bacteria (bacilli) in population is presented, where segmentation is performed using Marr Hildreth edge detector, then detection of beaded structure which characterizes the shape of individual bacteria is used for identification from cluster using probabilistic models. The algorithm is evaluated using, 2D images of bacilli cells of size 1040 × 1392 pixels. The results show a better count of segmented bacilli cells.

An approach based on active contour segmentation of about 1500 iterations is used in identification of rotavirus-A in [76]. After the segmentation of gray images, shape features like area, eccentricity, perimeter, circularity, length per width ratio and compactness are extracted and then identification is done by examining features if they are within max-min required ranges. 50 RGB digital images (resolution of 12-16 bits) of rotavirus-A particles (non-overlapping) taken from transmission electron microscopy are used for experiment. Finally this method yields an identification rate (accuracy) of 98.00%. The same method is applied in [77], for the analysis of spiral bacteria cell images, however, the classification is done using fuzzy classifier which yields an accuracy of 100%. During experiments, 1280 images containing three species of spiral bacteria are used (vibro spiral, spirochete and sprillium).

A method for segmentation and classification of large size images of zooplanktons is proposed in [78]. A split and merge active contour based method is used for segmentation. Firstly, images are split into tiles, then Otsu's is applied on each tile, after a morphological closing, a hough transform for circle detection is used to determine the starting contour points. Then active contour algorithm is executed on the binary image, finally, the tiles are merged before classification. In testing the algorithm, RGB images of zooplanktons of size 60000 × 60000 pixels are used. The segmentation approach is compared with longest contour and region growing approaches and the results show that the proposed active contour approach achieves the highest recall of 99.70%.

In [79], active contour based model (Chan-Vese (CV) model) is used in segmentation of Leishmania parasite in microscopic images, which is done after linear contrast and morphological operations. Segmentation is done in two ways, in the first approach termed as local method, images are split into small patches (masks) then segmentation is done on these patches while the other approach uses non split images and this way is termed as global method. During experiment, 20 RGB microscopic images of resolution 3246 × 2448 pixels containing Leishman parasites taken from bone marrow samples are used. The proposed method is compared with other Otsu, Sauvola and k-means segmentation methods. Better performance is achieved by the proposed method by an

accuracy of 89.10% and 90.24%, for global and local approaches, respectively.

In [80], a semi-automatic segmentation is used in content based analysis and classification of environmental microorganisms, in this approach segmentation is done using Sobel edge detector, followed by feature extraction in which four features are extracted (histogram descriptor, geometric feature, Fourier descriptor and internal structure histogram (ISH), then classification of each environmental microorganism is done using SVM, finally late fusion of outcomes of SVMs for each tested class of microorganism is done. In the experiments, 10 classes of environmental microoganisms (such as *Dicrmiphorus*, *Paramecinium* and *verticella*) are used with each class represented by 20 microscopic images. The proposed segmentation method achieves an accuracy of 98.70%. To increase the accuracy of the classification results, in [81] local features (SIFT) are additionally extracted and using the same segmentation and classification techniques, 20 images from each 15 classes of environmental microorganisms are used. This approach achieves the classification results of 97.70% accuracy. Furthermore, similar segmentation approach is applied in [82]–[85].

In [86], to tackle the hardship of segmentation on distorted images due to motion in waste water treatment systems, a Sobel edge detection method with multiple gradient thresholds is adopted to obtain better target edges, the proposed method is compared with conventional Sobel, Log and Canny edge based segmentation which are all done after image denoising. RGB microscopic images of microbacteria from waste water samples are used for experiment. The segmentation results produced by the proposed method and other compared methods are shown in Fig. 15.

Three segmentation methods of floc and filament in activated sludge waste water treatment plants are applied and evaluated in [87]. These methods are edge based segmentation (using Sobel), channel based segmentation using HSV format (global threshold is applied for segmentation), and Bradley thresholding method (in which local adaptive technique is used to generate binary image by thresholding local mean evaluated over a specific window size). RGB images of size 1224×960 pixels from activated sludge waste water samples are used during experiments. The segmentation results show that the edge based segmentation outperforms the other methods with an accuracy of 97.16%.

In [88], nine methods for segmentation of floc from phase contrast microscopic images of activated sludge (during monitoring of waste water treatment) are assessed. These methods are saturation color channel based approach, edge detection approach (Sobel based), k-means clustering algorithm, adaptive thresholding, texture based segmentation (Bradley adaptive thresholding), watershed algorithm, Kittler thresholding, split-merge approach and top-bottom-hat filtering based method. These methods are evaluated using, 61 RGB (phase contrast microscopic) images of size 1224×960 pixels captured from activated sludge. The evaluation results of the best four methods are considered. Among them edge based

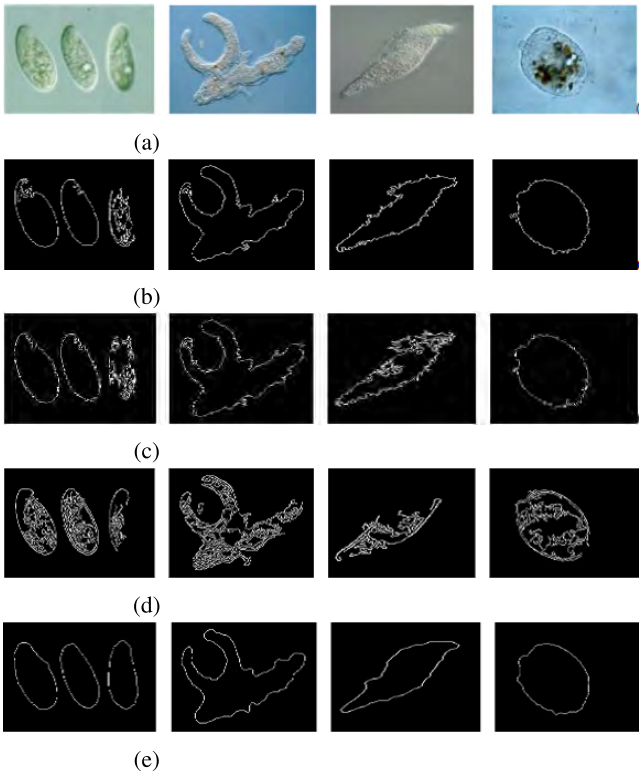

FIGURE 15. Contour extraction results with different edge detection algorithms. (a) original images, (b) Sobel, (c) Log, (d) Canny, (e) segmented images after multiple gradient thresholds method and edge connection [86].

method outperforms, with the highest accuracy of 99.70%, followed by watershed method with an accuracy of 99.67%.

To be able to segment filamentous algae in low contrast and noisy images in [89], segmentation results of two pipelines which focus on edge and region respectively, are combined using iterative erosion technique (region based ouput image is eroded several times to fit into edge based output segmentation results). The edge based approach involves, first, extraction of only blue channel (which shows distinct edges) from RGB, followed by adaptive thresholding on blue channel, then small unwanted objects are removed by morphological opening operation. The second approach which is proposed in [90], involves, Sobel edge detection, followed by canny which uses large smoothing parameter for roughly estimating the boundary of the elgae in image, then fine segmentation is achieved by applying Gaussian low pass filter of size 20×20 pixels and sigma of 0.5 in order to suppress the background and remain with foreground. In the experiments, 300 RGB images containing one among five species of filamentous algae (*Anabaena, Oscillatoria, Spirogyra, Spirulina, Anabaenopsis*) are used. The final segmentation results obtained are near to manual results.

D. SUMMARY OF CLASSICAL SEGMENTATION METHODS

A summary of the classical segmentation methodologies reviewed is given in Table. 1 in which, specific methods as applied to particular datasets from each work are indicated.

TABLE 1. Summary of reviewed works on classical based methods as applied to segmentation of microorganisms (threshold based segmentation methods (TBS), region based segmentation (RBS), edge based segmentation (EBS), used dataset type, dataset application field and quantity which include class (C), Total (T), training (Tr), validation (V), test (Te), positive (P), negative (N)).

Sub-category	Related works	Technique	Dataset (type, application field)	Quantity of dataset	Evaluation metrics
TBS	[41]	Objective threshold selection procedure (OTS)	Sphingomonas, medical	C=2	
TBS	[40]	Iterative selection	Biofilm, all	C=1	96.00% regression coefficient
TBS	[44]	Thresholding and morphological operations	Tuberculosis bacilli, medical	C=1, T=130, P=80, N=50	82.00% specificity
TBS	[43]	Otsu segmentation	Aureus and P.mirabilis, medical	C=2	
TBS	[48]	Global thresholding	C. elegans, science	C=1, T=5	83.00% accuracy
TBS	[45]	Global adaptive thresholding	Tuberculosis bacilli, medical	C=1, T=50	75.65% sensitivity
TBS	[46]	Color based thresholding	Tuberculosis bacilli, medical	C=1, T=55	
TBS	[33]	Adaptive color selection	Tuberculosis bacilli, medical	C=1, T=300	
TBS	[49], [50], [51]	Entropy thresholding	*Pseudomonas syringae, agriculture*	C=2, T=649	
TBS	[52]	Global thresholding	Spirillum, and Spirochete, bacteria	C=3, T= 1280	100.00 % accuracy
TBS	[53]	OTSU's optimal thresholding	Acinetobacter and Zygosaccharomyces, agriculture	C=2	
TBS	[54]	Global thresholding	C. elegans, science	C=1, T=150	
TBS	[55]	Trous wavelet transform	Hepatitis B virus, medical	C=1, T=40	80.00% accuracy
TBS	[56]	Global threshold	Tuberculosis bacilli, medical	C=1, T=25	99% accuracy
TBS	[57]	Mallat pyramid wavelet transform	Protozoa and metazoa, water treatment	C=1	
TBS	[58]	Thresholding	Green microalgae, enviromental	T=44	92.20% accuracy
TBS	[47]	Global thresholding	Tuberculosis bacilli, medical	C=1, T=50	
TBS	[13]	Otsu thresholding	Protozoa and metazoa, water treatment	C=1	
TBS	[59]	Otsu thresholding	Floc and filamentious bacteria, water treatment	C=1, T=40	98.50% accuracy
TBS	[60]	Color based thresholding	Plasmodium, medical	C=1, T=100	
TBS	[61]	Color based thresholding	Balantidium coli and Sarcocystis, medical	C=8, T=55	96.00% accuracy
RBS	[62]	Region grow	Bacillus subtilis , science	C=1	
RBS	[63]	Marker controlled watershed	Rotavirus-A, medical	C=1, T=50	
RBS	[64]	3D watershed	C. elegans, science	C=1	
RBS	[67]	Probabilistic framework	C. elegans, science	C=1, T=35	
RBS	[68]	H-Minima transform	Floc and filamentious bacteria, water treatment	C=1, T=30	
RBS	[65]	Region-growing watershed	Tuberculosis bacilli, medical	C=1, T=516	
RBS	[66]	Maker watershed	Tuberculosis bacilli, medical	C=1, T=50	83.84% accuracy
RBS	[69]	Concavity (MOC)	Overlapping bacilli, medical	C=1, T=100	
RBS	[70]	Watershed	Tuberculosis bacilli, medical	C=1, T=30, P=15, N=15	87.00% specificity
EBS	[72]	Minimum of the second derivative (MIND2)	Cryptophyte and Agellate	C=5, T=204	
EBS	[71]	Canny edge	Methanogenic bacteria, water treatment	C=2	
EBS	[73]	Canny edge	Tuberculosis bacilli, medical	C=1, T=472, P=75, N=397	100.00% sensitivity
EBS	[74]	Active Contour	Sphacelaria algae and Diatom aga, environmental	C=2	
EBS	[75]	Marr Hildreth edge detector	Pseudonoma aeruginosa, medical	C=1	
EBS	[76]	Active contour	Rotavirus-A, medical	C=1, T=50	98.00% accuracy
EBS	[77]	Active contour	Sprillium spiral bacteria, science	C=3, T= 1280	
EBS	[78]	Active Contour	Zooplankton, environmental	C=1	99.70% recall
EBS	[79]	Chan Vese (CV) model	Leishmania, medical	C=1, T=20	90.24% accuracy
EBS	[87]	Sobel	Lloc and filamentious bacteria, water treatment	C=1	97.16% accuracy
EBS	[80]	Sobel	Vorticella and Epistylis, environmental	C=10, T=200	98.70% accuracy
EBS	[81]	Sobel	Epistylis and Arcella, environmental	C=15, T=300	98.70% accuracy
EBS	[86]	Multiple gradient thresholds	Microbacteria, water treatment	C=1	
EBS	[88]	Sobel	Floc and filamentious bacteria, water treatment	C=1, T=61	99.70% accuracy
EBS	[89]	Multi-resolution edge detection	*Anabaena, Oscillatoria*, science	C=5, T=300	

In detail, types (name), species (classes), amount of datasets used and their related application fields such as medical, environmental and water treatment are indicated. To evaluate the strength of the applied techniques on tested dataset, segmentation results are given in accuracy (or other performance metrics if accuracy is not applicable in a reviewed work). As it can be observed from the table; most of the applied techniques have achieved an accuracy value higher than 82%. Thus they set a light to related researchers on most suitable, applicable and recent classical segmentation techniques for microorganisms. Moreover, it can be seen that, the most frequently used techniques are threshold based methods, this is because this major (threshold based) is comprised of many different alternatives such as global thresholding, Otsu, adaptive thresholding and multilevel thresholding. This gives a big room for segmenting and being suitable for many different segmentation challenges present on microorganim images. Furthermore, they are easy and direct to apply compared to other methods thus many researchers opt them for segmentation. A detailed analysis is given in Sec. IV-A on the most frequently used techniques and their advantages to segmentation of microorganisms.

III. MACHINE LEARNING METHODS FOR SEGMENTATION OF MICROORGANISMS

Machine learning is the scientific study of algorithms and statistical models that computer system uses to effectively perform a specific task without explicit instructions relying on patterns and inference. In this review machine learning based segmentation techniques are categorized as supervised machine learning (SML) and unsupervised machine learning (USML). Supervised learning algorithms build mathematical models from set of labeled data (images) which are used for training, and examples of SML algorithms are convolution neural networks, support vector machines and naïve Bayes models. USML algorithms build their mathematical models from set of data which contain only inputs and no desired output labels. The algorithms discover the data pattern and categorize them into groups. Typical examples of USML algorithms are k-mean and fuzzy c-means. An overview of some application methodologies, which are based on machine learning methods for microorganism image segmentation are given in subsections below.

A. SUPERVISED MACHINE LEARNING (SML)

In [11], a fully automated segmentation system for modeling and quantification of shape and motion of nematode *C. elegans* is introduced, where by assuming that the statistical properties of the background and foreground pixels remain unchanged during a time-lapse experiment, Neyman-peason model, which computes a likelihood ratio to classify the foreground pixels is applied to segment worms from background, then features for determining shape and motion are extracted. In the experiments, 16 image sequences representing four mutant stains of worms are used, with each sequence consisting of 150 frames at resolution of 1380×1032 pixels. Images consisting of overlapping worms are tested separately with non overlapping worms images. Finally, the segmentation accuracy for non overlapping and overlapping images obtained are 98.77% and 94.61%, respectively.

A supervised neural network is proposed in [91] to segment tuberculosis bacilli from ZN stained tissue. Since HSI color model has better representation capability, RGB to HIS conversion is done first, then these images are used for training and testing the network. Segmentation is done using hybrid multilayered perception (HMLP) neural network, which has been trained using modified recursive prediction error (MRPE) algorithm and uses sigmoid as activation function. 6802 images cropped at different sizes (42×54, 38×43, 50×56 and 800×600 pixels) are used for training and testing the network. This approach achieves impressive segmentation results with an accuracy above 97.75%, for all the tested groups.

In [92], a detection system to reduce false positive results in automatic detection of tuberculosis is proposed. In this system, the results of detection performed by support vector machine(referred to computer aided detection (CAD)) network are passed to stepwise binary decision classifier (SWC) for reduction of false positive (FP). In the experiments, 1803 TB positive and 6092 non TB positive images are used, and the results show the decrease in different types of false positive (FP) from CAD to SWC stages while optimizing true positive (TP).

A neural network is used for segmentation of urine sediments (bacteria, yeast and blood cells) from low contrast images [93], where a feed forward back propagation neural network is trained and tested using 24 bits RGB images of size 2048×1536 pixels containing urine sediments (bacteria, yeast, blood cells and other casts). The network is derived from the general least mean square (LMS) algorithm with only three layers. Experimental results show that, sediment counts obtained are almost similar to manual counts.

In [94], a segmentation algorithm for tuberculosis bacteria is applied so as to meet the WHO standard of fault diagnosis of less than 5.00%, where image contrast enhancement is done first, then RGB image intensities are found for all images, then training and evaluation of Naïve Bayes classifier is done using the intensities of RGB images as features. During performance evaluation of the proposed algorithm, 2063 RGB images taken from Ziehl-Neelsen sputum samples are used for training the classifier, then an accuracy value of 96.90% is obtained from the resultant confusion matrix.

In [95], an automatic segmentation and classification approach is applied to segment and classify human intestinal protozoa in feces. Due to the fact that most parasites are elliptical, the image segmentation step aims to locate candidate objects by ellipse matching and to define their spatial extent using image foresting transform technique (IFT), before IFT, image are enhanced by a Sobel gradient operator for an IFT- based object delineation. Then features are extracted and used to train and evaluate the optical path forest (OPF) classifier. In the experiments, 793 2D images containing

112 intestinal parasites and about 5142 impurities are used. Finally the segmentation accuracy of 98.22% is achieved.

An approach for segmentation and classification of bacteria is presented in [96]. Where, image patches containing only bacteria (foreground) of different species and others containing background with respective labels are used for training and testing a convolutional deep belief network (CDBN). CDBN is trained to obtain features for the preprocessed patches. Then a patch-level SVM model is trained to predict background or foreground, for the patches represented by the features resulted from training the CDBN. CDBN uses max pooling of size 2x2 which is small to make the model less sensitive to small shifts. Finally, patches detected as foreground are used to train and test the convolutional neural network (CNN) for classification. 862 images of size 128 × 128 pixels are used. The results of CNN are compared with k-NN and SVM (k-NN and SVM use SIFT features). The CNN outperforms the two other classification approaches with an accuracy of 62.10%.

In [97], two approaches for segmentation of TB bacteria from ZN stained samples are introduced. Feature vectors depicting 18 attributes for each pixel of the TB bacilli in the images, are applied to least mean square (LMS) and reduced rank with eigen decomposition algorithms separately, for segmentation. In the experiments, 80 RGB ZN stained images used. One image of size 684 × 912 pixels is used for training and 79 images of size 2736 × 3648 pixels are used for testing. The results of LMS and reduced rank algorithms are compared with segmentation results of classical methods and the proposed methods outperform with recall of 93.54% and 93.56% for LMS and reduced rank, respectively.

In [98], in order to overcome the problem of low number of dataset and noisy images of environmental microorganisms (EM), a weakly supervised learning system is proposed for segmentation and classification. Sparse coding method is applied for segmentation and feature extraction. It first learns a set of bases from random image patches, where each base represents a characteristic patch pattern. An image is then represented by a sparse linear combination of these bases, which captures high-level features of the image, and converts raw pixel values into an effective region-based representation (This resolves the shortage of less training images). Then the classification is accomplished using region based support vector machine (RBSVM) and finally late fusion is done to optimize classification results. In the experiments, 20 images which are taken from each of 15 classes of environmental microorganisms are used (example of classes are *Actinophrys*, *Arcella*, *Codosiga*, *Colpoda*, *Paramecium* and *Vorticella*). The proposed method for feature extraction and classification (NNSC and RBSVM) is compared with, bag of visual word features (BoVW) and linear SVM, the result of the proposed combination is more robust. Under the same context in [30], the DeepLab-VGG16 model is trained with EM images to generate pixel level features and global features, then these features are used to train the random forest (RF) classifier, then trained RF classifiers (for each image class) are used as the unary potentials by the conditional random field (CRF) model. Finally together with the pairwise potentials, the CRF model is applied to localize and label the objects of interest in the test environmental microscopic images. In the experiments, images from 20 EMs are used and 20 images are captured for each class. In order to evaluate the segmentation results, the proposed method for segmentation (local-global CRF) is compared with dense-CRF, denseCRF$_{org}$ (which uses DeepLab-VGG16 for segmentation) and full convolutional network (FCN). Finally the proposed method outperforms with an average accuracy of 94.20%.

In [99], a segmentation system is designed to monitor the algae in water bodies so as to get rid of harmful algal bloom, where image enhancement (sharpening) is applied first using multi-scale retinex filter, then SVM is trained on three prominent spacial features for segmentation. These features are mean and the standard deviation of all pixels on a small blocks and frequency of different areas in the image, which is calculated using wavelet transform technique. In the experiments, 200 images are used for training the classifier in which 100 images have algae only and other 100 have background only. The images include three species of algae, *Anabaena*, *Aphanizomenon* and *Microcystic*. The obtained results present an average detection rate (accuracy) of over 95.00%.

To overcome the scarcity of dataset in segmentation of bioimages, a CNN network is introduced in [100]. It is based on FCN however, it has five convolutional layers using PReLU, with one max pooling layer attached to the first layer, attached to the last layer is a deconvolutional layer, which upsamples the feature maps before it is given to a convsoftmax layer. The use of trainable deconvolutional layer enables segmentation accuracy of 97.30% on few tested dataset of C.elegans. To evaluate the performance of the proposed network, 76 notarized RGB images of size 501 × 501 pixels, with their corresponding binary ground truth are used for training, 19 for validation and 2 images for testing.

In [101], an automatic segmentation system is introduced to segment *Chaetoceros* marine phytoplankton, where pixel wise features are extracted using gray scale surface direction angle model (GSDAM), then segmentation is done using these features on a SVM. In the experiments, RGB images containing different species of *Chaetoceros* are used and the results are visually evaluated as in Fig. 16.

To enable classification of different stages of plasmodium vivax infected blood cells in [102], an object detection framework faster region-based convolutional neural network (Faster R-CNN) is used to detect objects red blood cell (RBC) vs non-RBC, by forming the bounding boxes. Then non-RBC objects are fed into AlexNet to classify them into seven categories (RBC, leukocyte, gametocyte, ring, trophozoite, and schizont). During experiments, 1300 RGB images of size 448 × 448 pixels are used for training, validation and testing. Comparing with human annotators, the proposed method achieves an accuracy of 98.00%.

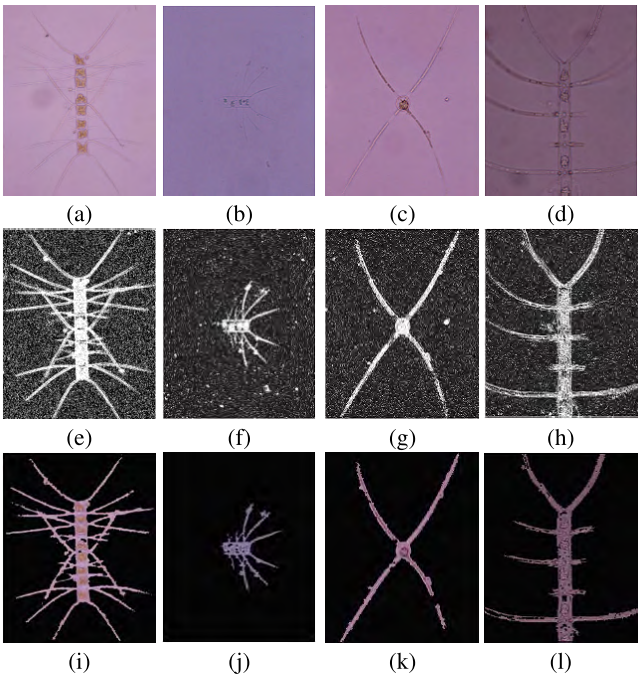

FIGURE 16. (a)–(d) Original *Chaetoceros* images. (e)–(h) segmented images after support vector machines and (i)–(l) the final segmentation results [101].

For successful segmentation of yeast cells in poor contrast and low illumination images captured from live cells in [103], a SegNet based neural network is deployed. In contrast to the original SegNet [36], the architecture input shape size used is $64 \times 64 \times 1$. To improve segmentation results training images are captured at different fluorescent modalities (DIC only, DIC 488 and DIC 561nm). In the experiments, 6000 2D image patches each containing single yeast cell are used for training while 1200, 1200 image patches are used for testing and validation. The result of 71.72% mean Intersection Union is obtained.

A fully convolutional network (FCN) is applied on identification of feline calicivirus in [104]. By varying the filter size of the first layer in 3×3, 5×5, 7×7, 9×9, and 11×11 size, the optimal size for better performance is found to be 7×7. The performance of FCN is improved monotonically with the increased filter size. However, larger filter sizes make the analyzed region narrower due to the characteristic of convolutional computation. The network is evaluated using 18 images of pixel size 128×128 for training and 17 for validation. The proposed FCN achieves results of 99.70% recall.

U-net based model is deployed in [105] to segment leishmania parasite. High-class imbalance in dataset is tackled by using generalized dice loss as loss function and adoption of two stage non uniform sampling scheme to select training patches. The network is first trained during some epochs (40 epochs) using patches that contain at least 40.00% of pixels from any of the three parasite classes (promastigote, amastigote, or adhered), then uniform sampling of all patches is used for the following epochs. From 45 dataset of size 224×224 pixels, 37 images are used for training. Results of 82.30% recall is achieved.

In [106], different segmentation methods are applied on extraction of objects from low contrast urine microscopic images, applied methods are unsupervised method (Sauvola's method as a key component), U-net method, unsupervised with edge thresholding, U-net with edge thresholding. In the experiments, 329 urine sample images are used. These images contain different types of urine objects such are bacteria, crystal, cast, epithelial cell, red blood cells, white blood cells and yeast. For training the U-net model, 4150 masks (patches) of size 64×64 pixels are manually generated from these 329 images.

In [107], a pyramid scene parsing (PSP) network (built on ResNet model) is applied in bacterial colony segmentation. To enlarge the receptive field of the network a set of dilated convolutions replaces standard convolutions in the ResNet part of the network. Then, a pyramid pooling module is used to gather context information, followed by both an upsampling and a concatenation layer, to form the final feature representation. During performance evaluation, 324 images of microbial Haemolysis are used, in which 221 images are used for training and 103 for testing the network. Finally, the segmentation accuracy above 98.00% is achieved.

A segmentation system for monitoring floc and filaments of activated sludge from phase contrast images is introduced in [108], where RGB to gray scale conversion is applied first, followed Gaussian low filter and finally segmentation is done using phase stretch transform (PST). With PST, image is converted to frequency (phase) domain by performing 2D fast Fourier transform (FFT), then to extract edges, phase image is binarized using one-level thresholding, the output is obtained by 2D IFFT. During experiments, 61 RGB phase contrast microscopic images of size 1224×960 pixels, taken from samples of water treatment plants are used. The proposed algorithm exhibits segmentation performance with an accuracy of 99.74%.

In [109], a convolution neural network based segmentation system is used to tackle the problem of insufficient dataset, where, augmentation is performed at angles 0, 90, 180, 270 degree to increase the datasets for training a U-net model. In order to train the model with the minimal annotated data, it is modified to use Dice coefficient as the loss function. In the experiments, 95 training images of rift valley virus are augmented by rotations and mirroring which resulted in 760 images. The images are of size 508×508 pixels. Finally the proposed CNN achieves the results of 90.00% dice score. Fig. 17 shows the proposed U-Net based CNN architecture.

In order to be able to segment protozoa image automatically, a region based convolutional model is proposed in [29]. In this approach segmentation is done using ResNet50 model and feature pyramid network (FPN) to produce segmentation masks then RetinaNet is used to identify species of protozoa. In the experiments, 38 images are used for training and 31 for testing (resolution of images vary from 824×941 to

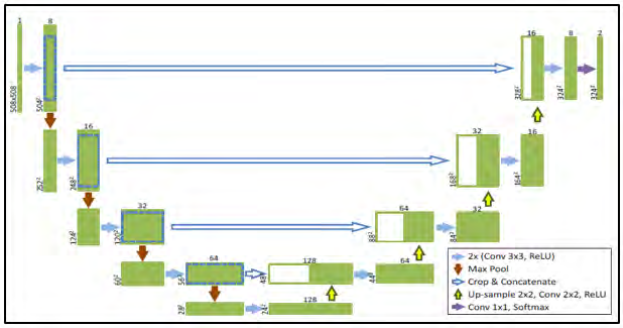

FIGURE 17. The U-Net-based CNN architecture [109].

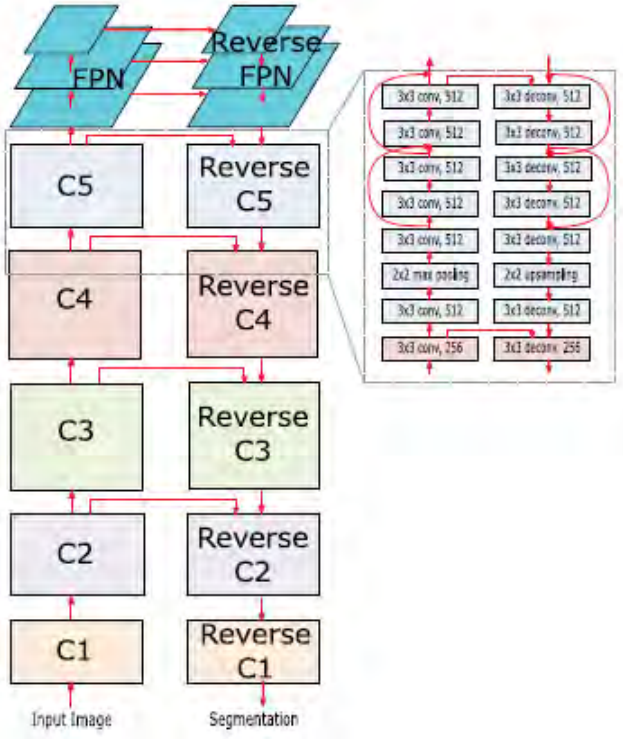

FIGURE 18. The architecture of FPN segmentation network with ResNet50 as the backbone [29].

4086 × 1725 pixels) and augmentation is used to increase the dataset by rotating images at intervals of 10 degree about the center of bounding boxes of protozoa images. Example of protozoa classes which are used for testing are *Giardia lamblia*, *Iodamoeba* and *Butschilii*. Evaluation of the proposed segmentation method is done using mAP which is the combination of precision and recall and maximum of 89.00% mAP is achieved. Fig. 18 shows the segmentation network.

B. UNSUPERVISED MACHINE LEARNING (USML)

In [110] a semi-automatic segmentation scheme for bacteria which takes into account each color separately is presented, where first RGB color separation is performed, then each color channel is converted to gray image and finally each color channel is segmented separately using adaptive neighborhood similarity comparison (spatial distance between each image pixel and its nearest point). In the experiments,

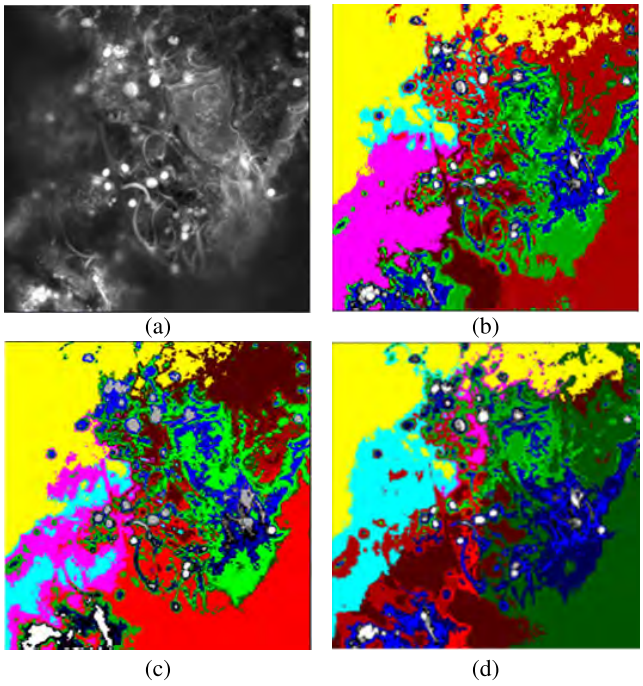

FIGURE 19. SOTM segmentation results, (a) original slice, (b) segmentation results when bxy = 0.01, (c) segmentation results when bxy = 0.02, (d) segmentation results when bxy = 0.1 [111].

16 RGB images containing different kind of bacteria are used. Average accuracy of 96.70% is achieved in finding the foreground objects of interest from all channels separately.

A self organizing tree map (SOTM) network is used to segment biofilms images so as to get insight of the internal parameters of the microbial in [111]. A set of features of 2D sample images are defined. These features are gray level (GL) of individual pixels, average gray level of a disk shaped region (GLdsk), phase congruency (PC) and position (XY) coordinates. The experiment is done in three different phases by changing criteria, first the network is allowed to grow to its maximum number of neurons up to 64, and by adding features one by one. Secondly, only XY features are varied where others are kept constant. Lastly dynamic features changes are allowed. The results show that few neurons are detected to represent the background and generally the results suggest that the SOTM can adaptively warp its topology into forms that reflect the type of segmentations typical to the human visual system. Fig. 19 shows the segmentation results by varying XY features.

In [112], a segmentation system to identify individual *C. elgans* from clusters of worms is presented, where segmentation of clusters from image is done first, by local adaptive thresholding and morphological opening followed by watershed segmentation and extensive merging. Then probabilistic model which is based on single worm to cluster area ratio and predefined path model, is applied to identify worms from clusters. In the experiments, 56 images each containing approximately 15 worms are used. The segmentation results are shown in Fig. 20.

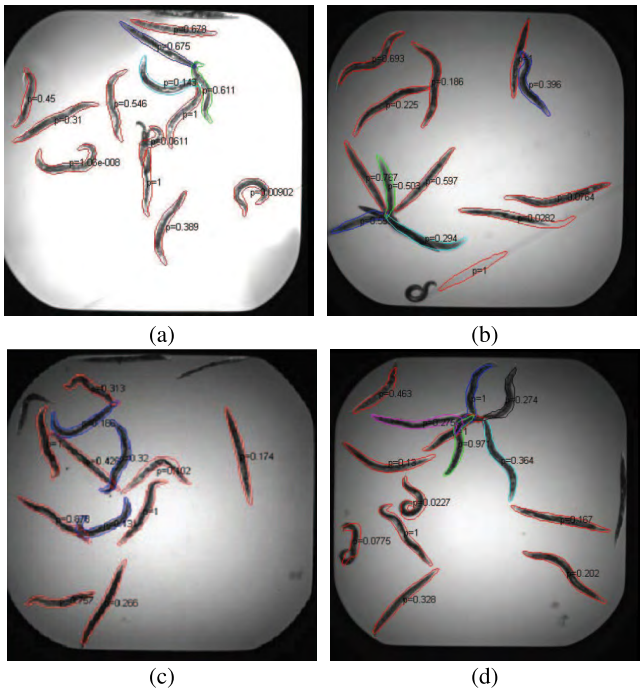

FIGURE 20. Cluster and single worms segmentation results of four sample images [112].

In [113], segmentation approach is proposed to segment TB bacilli from stained tissue images, where C-Y color model is used because of better mapping for luminance. Thus, Green and Ry channels of RGB and C-Y models respectively, are applied to moving k-mean clustering for initial segmentation (since bacilli are most highlighted and can clearly be seen in the green component of RGB and Ry component of C-Y color model), later a mean filter followed by region growing method are applied for fine segmentation. In the experiments, 30 to 50 RGB images from 25 tissue slides of TB positive samples are used and all images are further, categorized as normal, under-stained and over-stained images depending on the staining. The results of moving k-mean clustering above are used in [114] where, after segmentation median filter is used for denoising before Zemike moments features to be extracted, then classification takes place using hybrid multilayered perception network for detection of the bacilli. Finally the detection accuracy, sensitivity and specificity of 97.58%, 100% and 95.24% are obtained, respectively.

Plasmodium vivax segmentation system is proposed in [115], where the RGB to CMYk color conversion is performed and from this only C channel is selected as it is found that CMYk can give better presentation of the parasite in blood smear, then filtering is performed which is followed by segmentation using modified fuzzy divergence method which is based on Cauchy membership function, and capable of thresholding images with no distinct histogram valleys between background and foreground. Finally RGB color reconstruction is done to get the segmented RGB image. In the experiments, 150 RGB image frames of size 2048 × 1536 pixels captured from stained blood smears containing

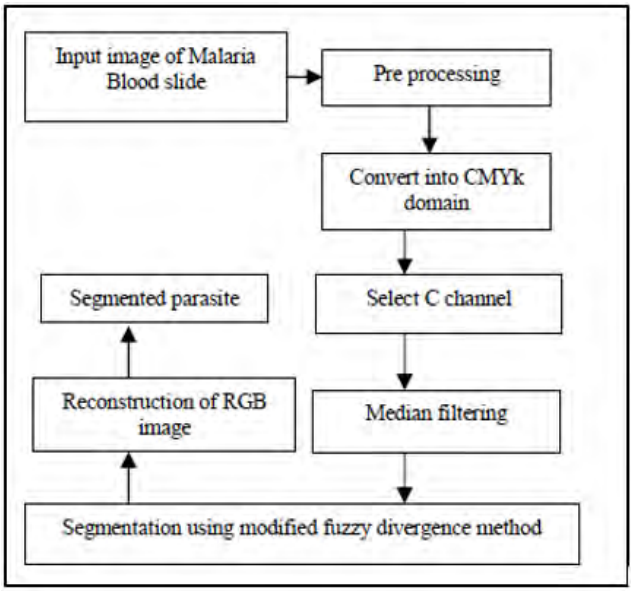

FIGURE 21. Fuzzy divergence based segmentation ([115]).

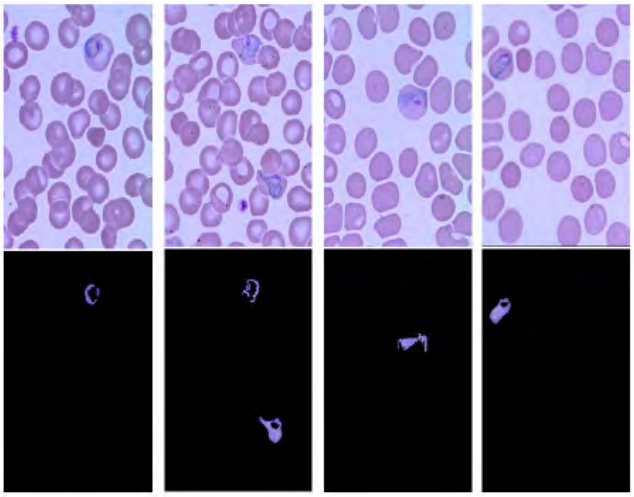

FIGURE 22. Top part of the figure shows the original images and down part of the figure shows segmented malaria parasites from rest of the background using fuzzy divergence method [115].

Plasmodium vivax are used. The flow chart for segmentation algorithm is shown in Fig. 21 and segmentation results are shown in Fig. 22.

In [116], evaluation of clustering and threshold segmentation techniques on tissue images containing TB bacilli is presented, where the performance of three clustering algorithms namely k-mean clustering, moving k-mean clustering and fuzzy c-mean clustering, and two adaptive thresholding algorithms, Otsu and iterative thresholding, are evaluated. 100 RGB images of TB positive sample tissues are used. These images are taken from variety of stained conditions termed as good, understained and overstained, then they are converted to C-Y color mode, and the saturation component is utilized as input to these algorithms, because it provides good separation between the TB bacilli and the background.

The achieved results show that k-mean clustering ($k = 3$) outperforms other methods with an accuracy of 99.49%.

In order to increase segmentation performance of microbe from bright field microscopic images, two approaches are evaluated on the use of condition random fields (CRF) technique before pixel wise classification (tree based Gaussian process classifier) stage in segmentation pipeline in [117]. First approach uses mean shift as unsupervised method, followed by pixel wise classifier decision (tree based Gaussian process classifier). Second approach uses extracted features and applies them on probabilistic Parzen classifier, followed by tree based Gaussian process classifier. In the experiments, RGB images of microbes are used, in which each image contains 40-470 microbes among the following *Bacillus subtilis*, *Escberichia coli*, *Micrococcus luteus*, *Staphylococcus epidermidis* and yeast. The obtained results show that both approaches increase performance with the use of CRF with an average accuracy of 80.00%.

In [118], a segmentation system of pulmonary tuberculosis bacteria is introduced. First, the image is resized to $n \times n$ square matrix, then it is divided into small square patches finally each patch is independently segmented using k-mean clustering and the results are stored in dictionary, then reconstruction of the segmented image is done from segmented patches. Images patches are used to avoid local minima problem which mostly face k-mean clustering. To evaluate the performance of the proposed method, 400 RGB images of size 640 $\times$ 360 pixels are used. Finally the segmentation accuracy of 97.68% is achieved.

In [119], segmentation and classification algorithm is applied so as to automate the TB diagnosis process. Segmentation is performed using fuzzy local information c-means (FLICM) clustering. FLICM is derived from fuzzy c-means clustering and it is an efficient algorithm, which is more robust to noise parameters (corrupted pixels) within an image, using its objective function, thus no any preprocessing is needed. After segmentation, features are extracted using Hu moments and SIFT algorithm and finally classification is done using least square support vector machines (LSSVM). In the experiments, 299 images (512 $\times$ 512 pixels) captured from ZN stained sputum under digital microscope are used. The results of 95.10% accuracy, is achieve for segmentation.

A segmentation system capable of segmenting 3D images containing bacteria biofilms is introduced in [120], where in order to identify and segment the individual bacteria in 3D, each layer of 3D image is segmented differently using Bact-3D algorithm and finally reconstruct the segmented 3D volume as shown in Fig. 23. The performance of the proposed algorithm, is tested using 3D biofilm images and an accuracy of 99.81% is obtained.

In [121], an automatic segmentation method is used to detect malaria parasites from stained blood smears containing four types of *Plasmodium* (*falciparum, malariae, ovale* and *vivax*). The algorithm uses green channel which is dominant channel for plasmodium in RGB image, then Gamma correlation is applied for image enhancement, followed by noise removal by Gaussian filter, then edge enhancement and fuzzy c-means clustering are applied for segmentation. The final segmentation results achieve an accuracy of 98.26%.

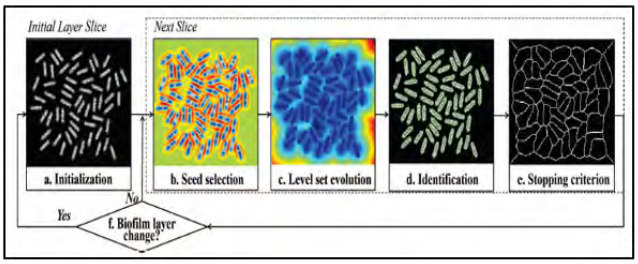

FIGURE 23. Flow chart of Bact-3D algorithm [120].

In order to effectively segment TB bacteria from microscopic images of sputum samples, a clustering based method is presented in [122]. Where an improved fuzzy local information c-means (IFLICM) clustering, is used for segmentation. IFICM is capable to combine both local spatial and local gray level information in a fuzzy way to preserve robustness and noise insensitiveness. It manages the effect of neighborhood pixels depending on their distance from the central pixel. It is derived and improved from fast generalized fuzzy c-means and fuzzy c-means algorithms. During experiments, 99 RGB images of ZN stained bacilli are used in which, 29 of them are resized into 512$\times$512 pixels and used for training the system and 70 images are used for testing. The performance accuracy of 96.05% is achieved.

Although, to the best of our knowledge, generative adversarial networks (GANs) have never been applied directly to segmentation of microorganisms, they show great potential in enhancing segmentation of microscopic images, which share similar characteristics and segmentation challenges as microorganisms. Such as segmentation of prostate cancer cells from low contrast images and synthesis of more dataset to tackle the challenge of scarcity in dataset, especially in deep learning related segmentation methods [28], [123]. Thus, a brief overview on GANs with related works is given in Sec. IV-D.

C. SUMMARY OF MACHINE LEARNING METHODS

A summary of machine learning based methods investigated in this review is given in Table 2. It indicates, specific segmentation techniques and datasets (types, species, amount and their related application fields) from each investigated work. To evaluate the significance of the applied technique on the datasets, experimental results are also indicated (in accuracy or other metrics, if accuracy in not applicable). General assessment shows that, most of the applied methods have achieved accuracy higher than 80%. Thus, they set a light to related researchers on the most suitable, recent and applicable techniques for segmentation of microorganisms. Furthermore, it can be observed that, the most frequent used methods are supervised learning methods especially neural network based models. This is because with neural network models significant hierarchical relationships within data can

be discovered algorithmically without laborious hand craft features. A detail analysis is given in Sec. IV-B on the most frequently used techniques and their advantages to specific segmentation challenges on microorganism images.

IV. METHODOLOGY ANALYSIS

Many techniques have been applied in segmentation of microoganisms, however, some have emerged to be more prominent than others in both classical and machine learning based methods as discussed in subsections below.

A. ANALYSIS ON CLASSICAL METHODS

In classical methods, as observed in Table. 1, threshold based segmentation (TBS) methods are the most frequently used techniques, this is because threshold based segmentation has many alternatives such as global, multithreshold, Otsu and adaptive thresholding. This accounts for it being suitable for many different segmentation challenges present in microorganism images. For example, most of microscopic images have uneven illumination on the backgrounds due to the nature of environments where microorganisms are found, under this case adaptive and multithreshold techniques are suitable (adaptive thresholding uses different threshold values for different local areas on image) [38].

Low (poor) contrast ratio between background and foreground, is also a big challenge faced in microorganism images [55], in which histogram of images have no clear defined valley point for thresholding. This challenge mostly appears to images from conventional light microscopes which are commonly used in many third world countries [40], [45], however, this can be resolved using iterative thresholding [124], wavelet transform [55] and color based thresholding. A clear example can be seen in [45] where color and global adaptive thresholding are used to threshold low contrast image from conventional microscope. In most cases when staining is applied to the tested sample then capturing images, the foreground and background are sufficiently distinct, in this case global, histogram based and Otsu thresholds are suitable for segmentation. For example in [43] Otsu thresholding is applied on stained sample images, in [56] and [48] global thresholding is applied on stained sample images.

Moreover, threshold based techniques are the easiest methods to implement. This is why they are mostly used [125]. Furthermore, they don't require many datasets, thus suitable for segmentation of medical related microorganisms where confidentiality leads to scarcity of dataset [45], [46], [55]. On top of that, threshold based methods have simple algorithms which can be run by low speed computers and are incorporated in software libraries which can be utilized by almost all common programming languages and platforms, such as python and Matlab, contrary to many machine learning models which need high speeds, high number of dataset and can run well only in some special IDEs. For example in [43], [52], [59] Matlab is used during experiments. Additionally, threshold segmentation techniques are generally inexpensive and computationally faster [126]. All these make threshold based methods being suitable for most of segmentation challenges in microorganism images.

B. ANALYSIS ON MACHINE LEARNING BASED METHODS

In machine learning based methods as illustrated in Table. 2, supervised machine learning (SML) methods are the most frequently used ones, especially in recent years they have emerged to be very prominent. Among machine learning methods, neural network related methods are the most frequently used, this is because, with neural network, significant hierarchical relationships within the data can be discovered algorithmically without laborious hand crafted features [127], thus it is easier to apply them for segmentation than other machine learning methods like SVM, which need prior hand crafted features. Moreover, because of the recent innovation of high speed computers which can handle bulk dataset and complex neural network algorithms (as seen from table 2, that most of the deep learning based techniques have been applied in recent years 2015–2018).

Neural network based models are non linear models which are able to capture non-linear and complex underlying characteristics of images with high degree of accuracy, this gives them capability to handle most of segmentation challenges in microorganism images such as, uneven illumination, poor contrast and non uniform undesired small features on microorganim images [81], [103], [106].

Another challenge on microorganim images is scarcity of dataset. However, with augmentation technique enough dataset can be generated from few present dataset and applied to neural network models for better segmentation results, for example in [109] and [29] augmentation is applied to increase the dataset for training. Moreover, the application of transfer learning has boosted the use of neural network models in the segmentation of microorganisms, for example the application of transfer learning can be seen in [30] where VGG-16 model is used, in [29] where ResNet50 model is used and in [106], [109], where U-net model is used for segmentation. Therefore, many of the recent works are focusing on application of neural networks.

C. POTENTIAL RELATED FIELDS FOR APPLICATIONS OF SIMILAR SEGMENTATION METHODS

Segmentation techniques discussed in this paper are not only suitable for microorganism images, but find application in other related fields such as, in sperm cell segmentation and detection. Sperm cell microscopic images share many similar segmentation challenges with microorganism images including, poor contrast and small size of the foreground related to background. Therefore, same segmentation techniques can be applied in both tasks. Particular examples are, identification of acrosome and nucleus in sperm cells [128], identification of bovine sperm head for morphometry analysis in quantitative phase contrast holographic [129], low contrast sperm tracking [130] and rat sperm image segmentation and counting [131]. Moreover,

TABLE 2. Summary of reviewed works on machine learning based methods (supervised machine learning (SML), unsupervised machine learning (USML), used dataset type, dataset application field and quantity which include class (C), Total (T), training (Tr), validation (V), test (Te), postive (P), negative (N)).

Sub-category	Related works	Technique	Dataset (type, application field)	Quantity of dataset	Evaluation metrics
SML	[11]	Neyaman peason model	C. elegans, science	C=4, T=2400	98.77% accuracy
SML	[91]	Hybrid multilayered perception (HMLP) NN	Tuberculosis bacilli, medical	C=1, T=6802	97.75% accuracy
SML	[92]	Stepwise binary decision classifier (SWC)	Tuberculosis bacilli, medical	C=1, T=7895, P=1803, N=6092	
SML	[94]	Naive bayes classier	Tuberculosis bacilli, medical	C=1, T=2063	96.90% accuracy
SML	[93]	Feed forward back propagation neural network	Yeast cell, medical	C=1	
SML	[95]	Foresting transform method (IFT)	Protozoa, medical	C=15, T=793	98.22% accuracy
SML	[96]	Convolution neural network (CNN)	Bacterial colony, science	C=1, T=862	62.10% accuracy
SML	[98]	Sparce coding	Epistylis and Rotifera, environmental	C=15, T=300	
SML	[99]	Support vector machine	Aphanizomenon and Microcystic, water treatment	C=3, T=200	95.00% accuracy
SML	[97]	Least mean squares (LMS)	Tuberculosis bacilli, medical	C=1, T=80, Tr=79, Te=1	93.54% recall
SML	[100]	Fully convolutional network (FCN)	C. elegans, science	C=1, T=97, Tr=76, V=19,Te=2	97.30% accuracy
SML	[101]	Support vector machine	Chaetoceros, environmental	C=1	
SML	[102]	Faster region-CNN	*Pasmodium vivax, medical*	C=1, T=1300	98.00% accuracy
SML	[103]	SegNet model	Yeast cell, medical	C=1, T=8400, Tr=6000, V=1200, Te=1200	71.72% mean intersection union
SML	[104]	Fully convolutional network (FCN)	Feline calicivirus, medical	C=1, T=35, Tr=18, V=17	99.70% recall
SML	[105]	U-net model	Leishmania, medical	C=1, T=45, Tr=37, V=8	82.30% recall
SML	[106]	U-net model	Yeast cell, medical	C=1, T=329	
SML	[107]	Pyramid scene parsing (PSP) network	Microbial colony, medical	C=1, T=324, Tr=221, V=103	98.00% accuracy
SML	[109]	CNN (U-Net architecture)	Rift valley virus, medical	C=1, T=4138, Tr=4000, V=138	90.00% dice score
SML	[108]	Phase stretch transform (PST)	Floc and filament bacteria, water treatment	C=1, T=61	99.74% accuracy
SML	[30]	VGG-16 and Condition random Field	Aspidisca and Codosiga, environmental	C=20, T=400	94.20% accuracy
SML	[29]	ResNet50 and Feature pyramid network	Giardia lamblia and Iodamoeba butschili protozoa, medical	C=1, T=69, Tr=38, Te=31	89.00% mAP
USML	[110]	Adaptive neighbourhood similarity comparison	Bacteria, medical	C=1, T=16	96.70% accuracy
USML	[111]	Self organising tree map (SOTM) network	Biofilm, All	C=1	
USML	[113], [114]	Moving k-mean clustering	Tuberculosis bacilli, medical	C=1, T=50	
USML	[112]	Probabilistic shape model	C. elegans, science	C=1, T=56	
USML	[115]	Fuzzy divergence method	Plasmodium vivax, medical	C=1, T=150	
USML	[116]	k-mean clustering	Tuberculosis bacilli, medical	C=1, T=100	99.49% accuracy
USML	[117]	Condition random fields	Bacillus subtilis, medical	C=5	80.00% accuracy
USML	[118]	k-mean clustering	Tuberculosis bacilli, medical	C=1, T=400	97.68% accuracy
USML	[119]	Fuzzy local information c-Means (FLICM) clustering	Tuberculosis bacilli, medical	C=1, T=299	95.10% accuracy
USML	[120]	BACT -3D	biofilm, All	C=1	99.81% accuracy
USML	[122]	Improved fuzzy local information c-means (IFLICM) clustering	Tuberculosis bacilli, medical	C=1, T=99, Tr=29, Te=70	96.05% accuracy
USML	[121]	Fuzzy c-means clustering	Plasmodium , medical	C=4, T=574	98.26% accuracy

the discussed segmentation techniques find potential application in cytopathology and histopathology images when image segmentation is done under cellular level. As these images share some similar characteristics and segmentation challenges with microorganisms such as, overlapping of cells, poor contrast for non stained sample images, superposition of different colors due to unideal distribution of stains on the reaction regions and variation of illumination over the background. Specific examples are, cluster detection in cytology images [132], automatic screening of cytological specimens [133], breast cancer detection and diagnosis [134], [135], segmentation of epithelial cervical cells in images [136], image segmentation of overlapping cervical cells [137], image guided fine needle aspiration

of retroperitoneal masses [138], segmentation of cervical and breast clustered cells from histopathology images [139], detection of mitosis and karyorrhexis cells in digitized histological images in prognosis of neuroblastoma [140], segmentation of immunohistochemical tissue images [141], nucleus discrimination in microscopy images of diffuse glioma [142] and segmentation of clustered nuclei from bone marrow and peripheral blood specimens images to perform a non-isotopic *in situ* hybridization of their DNA content [143].

D. OTHER POTENTIAL METHODS FOR SEGMENTATION OF MICROORGANIMS

Generative adversarial networks (GANs) based segmentation methods have shown a great potential in segmentation of microscopic images, which share similar segmentation characteristics as microorganisms. GAN is a machine learning network having two models which work in adversarial manner [144]. It is composed of a generative model that captures the data distribution and a discriminative model that estimates the probability that a sample came from training data rather than generator [144]. The generative network training objective is to increase the error rate of the discriminative network [145]. The architectural constraints of GANs have demonstrated that they are strong candidates for unsupervised learning. In the context of unsupervised learning, generative adversarial network (GAN) can be trained on unlimited amount of unlabelled images to learn their intermediate representations [146]. Incorporating them into image segmentation tasks for microscopic images, has shown great improvement in segmentation results. Some successful applications of GANs to microscopic images segmentation tasks are briefly introduced below:

Motivated by the fact that, image translation shown by GAN loss can improve the blurred quality of image to image translation generated by U-net [27], a dual contour adversarial network (DCANet) is used for segmentation of nucleii from pathological images of cancer tissue in [147]. In this network, a generator deploys two decoding lines which generate two image masks with different boundary transformation, then both images are post-processed using maker watershed before combining them to form a segmented image. Comparing with linkNet, FnsNet and Pix2Pix on segmentation of the same dataset, the proposed method outperforms with F1 score of 70.00%.

A deep adversarial network for biomedical image segmentation (utilizing unannotated images) is applied on stained colon tissue images [148], for glands segmentation. An evaluation convolution network (VGG-16 model) is encouraged to distinguish between segmentation results of unannotated images and annotated ones (by giving them different scores). While a segmentation network is encouraged to produce segmentation results of unannotated images such that evaluation network cannot distinguish them from the annotated ones.

In [28], a GAN is used in synthesizing data for aggressive prostate cancer detection, to tackle the scarcity of data set for training the fully convolutional network (FCN). The generator of GAN consists of the U-net-type architecture. It uses InsanceNorm layers instead of BatchNorm layers, conjecturing that it avoids harmful stochasticity introduced by small batch-sizes. The discriminator is similar to encoder of the generator. A sensitivity of 98.00% is achieved in segmentation.

A convolutional network which works in the principle of GAN is applied to segment proteomics of individual cancer cells in [149]. Unlike the original GAN, this network doesn't generate images from random noise vectors, rather estimates the underlying variables of an image. The estimator learns to output some segmentation of the image while the discriminator learns to distinguish between expert manual segmentations and estimated segmentations given the associated image. (The estimator net is a five layer fully CNN, each layer is constructed of a convolution followed by batch normalization and leaky-ReLU activation. The discriminator is designed as three consecutive ''Rib Cage'' blocks followed by two fully-connected (FC) layers with leaky-ReLU activations and a final FC layer with one output and a sigmoid activation for classification). With this network the loss function is automatically defined as it is learned along side the estimator, making this a simple to use algorithm with no tuning necessity and it is robust to low number of training samples. The final segmentation result of 89.90% precision is achieved.

Generally, similar approaches based on GANs can be applied in segmentation of microorganisms. Since they share some similar segmentation challenges with cancer cells, such as uneven illumination of backgrounds which are the results of poor staining of samples [26], [147], poor contrast [123] and scarcity of dataset [28].

V. CONCLUSION AND FUTURE WORK

In this review, an overview on microorganism image segmentation approaches is given, where they are grouped into classical and machine learning based methods. Furthermore, they are subcategoried into threshold, region and edge based methods which belong to classical methods, supervised and unsupervised methods which belong to machine learning based methods. In each of the subcategories, related works are reviewed in an ascending time line. From classical review works in Sec. II and subsequent analysis in Sec. IV-A, it is found that threshold based methods are the most frequently used among all classical methods due to their suitability to many segmentation challenges in microorganim images as highlighted in Sec. IV. Among machine learning based methods whose related works and corresponding analysis are discussed in Sec. III and IV-A, supervised learning methods particularly neural network based methods, are the most frequently applied ones and have shown abrupt increase of their applications since 2015. This is due to, their suitability to many microorganism segmentation challenges and ability to capture significant relationship within images without laborious hand crafted features.

TABLE 3. Related reviewed works, categories, subcategories and publication year. Categories are classical and machine learning (ML). Subcategories are threshold based segmentation (TBS), region based segmentation (RBS), edge based segmentation (EBS), supervised machine learning (SML), unsupervised machine learning (USML).

Category	Subcategory	Year	Research team	Related works
Classical	TBS	1994	M. Dubuisson	[71]
Classical	TBS	2001	J. Xavier	[41]
Classical	TBS	2001	X. Yang	[40]
Classical	TBS	2003	M. Forero	[44]
Classical	TBS	2007	J. Yerly	[43]
Classical	TBS	2008	M. Costa	[45]
Classical	TBS	2008	R. Raof	[46]
Classical	TBS	2009	V. Makkapati	[33]
Classical	TBS	2009 -2011	D. Rojas	[50], [49], [51]
Classical	TBS	2011	P. Hiremath	[52]
Classical	TBS	2011	H. Kim	[53]
Classical	TBS	2012	P. Rodrigues	[54]
Classical	TBS	2012	F. Levet	[55]
Classical	TBS	2013	H. Rachana	[56]
Classical	TBS	2014	Y. Wang	[57]
Classical	TBS	2015	V. Borges	[58]
Classical	TBS	2015	M. Wahidah	[47]
Classical	TBS	2015-2016	M. Khan	[13], [59]
Classical	TBS	2017	E. Haryanto S	[60]
Classical	TBS	2018	K. Pho	[61]
Classical	RBS	2006	E. Battenberg	[62]
Classical	RBS	2010	P. Hiremath	[63]
Classical	RBS	2012	F. Long	[64]
Classical	RBS	2014	A. Greenblum	[67]
Classical	RBS	2014	X. Lee	[68]
Classical	RBS	2014	M. Chayadevi	[65]
Classical	RBS	2014	C. Xu	[66]
Classical	RBS	2015	E. Priya	[69]
Classical	RBS	2016	M. Shahl	[70]
Classical	EBS	1989	M. Sieracki	[72]
Classical	EBS	2002	M. Vargas	[73]
Classical	EBS	2006	M. DaneshPanah	[74]
Classical	EBS	2008	N. Rizvandi	[48]
Classical	EBS	2010	P. Vallotton	[75]
Classical	EBS	2011-2012	P. Hiremath	[76], [77]
Classical	EBS	2014	E. Gutzeit	[78]
Classical	EBS	2015-2017	C. Li	[80], [81], [82], [83], [84], [85]
Classical	EBS	2015	M. Arahi	[79]
Classical	EBS	2016	H. Nisar,	[87]
Classical	EBS	2016	F. Zhou	[86]
Classical	EBS	2017	M. Khan	[88]
ML	SML	2005	M. Kyan	[111]
ML	SML	2007	N. Roussel	[11]
ML	SML	2010	M. Osman	[114], [91]
ML	SML	2011	C. Pangilinan	[92]
ML	SML	2012	R. Rulaningtyas	[94]
ML	SML	2012	W. Maneesukasem	[93]
ML	SML	2013	C. Suzuki	[95]

TABLE 3. ***(Continued.)*** **Related reviewed works, categories, subcategories and publication year. Categories are classical and machine learning (ML). Subcategories are threshold based segmentation (TBS), region based segmentation (RBS), edge based segmentation (EBS), supervised machine learning (SML), unsupervised machine learning (USML).**

ML	SML	2015	C. Li	[98], [150]
ML	SML	2015	D. Nie	[96]
ML	SML	2015	K. Dannemiller	[99]
ML	SML	2015	V. Ayma	[97]
ML	SML	2016	S. Wiehman	[100]
ML	SML	2016	X. Qiu,	[101]
ML	SML	2017	J. Hung	[102]
ML	SML	2017	S. Aydin	[103]
ML	SML	2018	E. Ito	[104]
ML	SML	2018	G. Marc	[105]
ML	SML	2018	A. Aziz	[106]
ML	SML	2018	P. Andreini	[107]
ML	SML	2018	D. Matuszewski	[109]
ML	SML	2018	R. Ang	[108]
ML	SML	2018	S. Kosov	[30]
ML	SML	2018	K. Pho	[61]
ML	USML	2004	C. Reddy	[110]
ML	USML	2010-2012	M. Osman	[113], [116]
ML	USML	2010	C. Wahlby	[112]
ML	USML	2011	M. Ghosh	[115]
ML	USML	2013	M. Kemmler	[117]
ML	USML	2015	R. Rulaningtyas	[118]
ML	USML	2017	K. Mithra	[119], [122]
ML	USML	2017	J. Wang	[120]
ML	USML	2017	Y. Hendrawan	[121]

Thus, from the technical capability analysis and development trend of image segmentation techniques on microorganisms, we suppose the on going application of the discussed segmentation methods especially the most frequently used ones (particularly neural network based models, self built and by transfer learning) not only to microorganism images but also in other related fields such as cervical cancer cells segmentation, sperm cell segmentation, cytopathology and histopathology image segmentation which share similar image characteristics.

APPENDIX
GENERAL OVERVIEW OF APPLIED METHODS FOR SEGMENTATION OF MICROORGANISMS, LISTED CHRONOLOGICALLY

See Table. 3.

ACKNOWLEDGMENT

The authors would like to thank M. E. Patrice Monkam for his proof reading work and Miss Zixian Li for her important discussion.

REFERENCES

[1] O. O. Babalola, "Beneficial bacteria of agricultural importance," *Biotechnol. Lett.*, vol. 32, no. 11, pp. 1559–1570, 2010.

[2] N. R. Pal and S. K. Pal, "A review on image segmentation techniques," *Pattern Recognit.*, vol. 26, no. 9, pp. 1277–1294, 1993.

[3] J. Bezdek, L. Hall, and L. Clarke, "Review of MR image segmentation techniques using pattern recognition," *Med. Phys.*, vol. 20, no. 4, pp. 1033–1048, 1993.

[4] V. Dey, Y. Zhang, and M. Zhong, "A review on image segmentation techniques with remote sensing perspective," in *Proc. 7th Symp. Int. Soc. Photogramm. Remote Sens. (ISPRS)*, 2010, pp. 31–42.

[5] C. Li, N. Xu, T. Jiang, S. Qi, F. Han, W. Qian, and X. Zhao, "A brief review for content-based microorganism image analysis using classical and deep neural networks," in *Proc. Int. Conf. Inf. Technol. Biomed.*, 2018, pp. 3–14.

[6] M. Madigan, K. S. Bender, D. H. Buckley, W. M. Sattley, and D. A. Stahl, *Brock Biology of Microorganisms*. Upper Saddle River, NJ, USA: Prentice-Hall, 1997.

[7] Q. Zhou, K. Li, X. Jun, and L. Bo, "Role and functions of beneficial microorganisms in sustainable aquaculture," *Bioresource Technol.*, vol. 100, no. 16, pp. 3780–3786, 2009.

[8] S. Rossetti, M. Tomei, P. H. Nielsen, and V. Tandoi, "*'Microthrix parvicella'*, a filamentous bacterium causing bulking and foaming in activated sludge systems: A review of current knowledge," *FEMS Microbiol. Rev.*, vol. 29, no. 1, pp. 49–64, 2005.

[9] D. Pryce, "Sputum film cultures of tubercle bacilli: A method for the early observation of growth," *J. Pathol. Bacteriol.*, vol. 53, no. 3, pp. 327–334, 1941.

[10] M. Forero, F. Sroubek, and G. Cristóbal, "Identification of tuberculosis bacteria based on shape and color," *Real-Time Imag.*, vol. 10, no. 4, pp. 251–262, 2004.

[11] N. Roussel, C. A. Morton, F. P. Finger, and B. Roysam, "A computational model for C. elegans locomotory behavior: Application to multiworm tracking," *IEEE Trans. Biomed. Eng.*, vol. 54, no. 10, pp. 1786–1797, Oct. 2007.

[12] C. Zhang, W.-B. Chen, W.-L. Liu, and C.-B. Chen, "An automated bacterial colony counting system," in *Proc. IEEE Int. Conf. Sensor Netw., Ubiquitous, Trustworthy Comput.*, 2008, pp. 233–240.
[13] B. Khan, H. Nisar, A. Ng, K. Lo, and V. Yap, "Local adaptive approach toward segmentation of microscopic images of activated sludge flocs," *J. Electron. Imag.*, vol. 24, no. 6, p. 061102, 2015.
[14] K. S. Fu and J. K. Mui, "A survey on image segmentation," *Pattern Recognit.*, vol. 13, no. 1, pp. 3–16, 1981.
[15] J. Canny, "A computational approach to edge detection," in *Readings in Computer Vision*. Amsterdam, The Netherlands: Elsevier, 1987, pp. 184–203.
[16] M. Kass, A. Witkin, and D. Terzopoulos, "Snakes: Active contour models," *Int. J. Comput. Vis.*, vol. 1, no. 4, pp. 321–331, 1988.
[17] D. Marr and E. Hildreth, "Theory of edge detection," *Proc. Roy. Soc. London. B, Biol. Sci.*, vol. 207, pp. 187–217, Feb. 1980.
[18] N. Otsu, "A threshold selection method from gray-level histograms," *IEEE Trans. Syst., Man, Cybern.*, vol. 9, no. 1, pp. 62–66, Jan. 1979.
[19] S. Beucher, "Watersheds of functions and picture segmentation," in *Proc. IEEE Int. Conf. Acoust., Speech, Signal Process. (ICASSP)*, May 1982, pp. 1928–1931.
[20] H. Xu, G. Zhu, J. Tian, X. Zhang, and F. Peng, "Image segmentation using support vector machine," *Proc. SPIE*, vol. 6044, p. 60441U, Nov. 2005.
[21] E. E. Osuna, "Support vector machines: Training and applications," Ph.D. dissertation, Massachusetts Inst. Technol., Cambridge, MA, USA, 1998.
[22] J. Long, E. Shelhamer, and T. Darrell, "Fully convolutional networks for semantic segmentation," in *Proc. IEEE Conf. Comput. Vis. Pattern Recognit.*, Jun. 2015, pp. 3431–3440.
[23] O. Ronneberger, P. Fischer, and T. Brox, "U-net: Convolutional networks for biomedical image segmentation," in *Proc. Int. Conf. Med. Image Comput. Comput.-Assist. Intervent*, 2015, pp. 234–241.
[24] J. C. Bezdek, W. Full, and R. Ehrlich, "FCM: The fuzzy c-means clustering algorithm," *Comput. Geosci.*, vol. 10, nos. 2–3, pp. 191–203, 1984.
[25] A. K. Jain, "Data clustering: 50 years beyond K-means," *Pattern Recognit. Lett.*, vol. 31, no. 8, pp. 651–666, 2010.
[26] L. Hou, A. Agarwal, D. Samaras, T. M. Kurc, R. R. Gupta, and J. H. Saltz, "Unsupervised histopathology image synthesis," 2017, *arXiv:1712.05021*. [Online]. Available: https://arxiv.org/abs/1712.05021
[27] P. Isola, J.-Y. Zhu, T. Zhou, and A. A. Efros, "Image-to-image translation with conditional adversarial networks," in *Proc. IEEE Conf. Comput. Vis. Pattern Recognit.*, Jul. 2017, pp. 1125–1134.
[28] S. Kohl, D. Bonekamp, H.-P. Schlemmer, K. Yaqubi, M. Hohenfellner, B. Hadaschik, J.-P. Radtke, K. Maier-Hein, "Adversarial networks for the detection of aggressive prostate cancer," 2017, *arXiv:1702.08014*. [Online]. Available: https://arxiv.org/abs/1702.08014
[29] K. Pho, M. Amin, and A. Yoshitaka, "Segmentation-driven retinanet for protozoa detection," in *Proc. IEEE Int. Symp. Multimedia (ISM)*, Dec. 2018, pp. 279–286.
[30] S. Kosov, K. Shirahama, C. Li, and M. Grzegorzek, "Environmental microorganism classification using conditional random fields and deep convolutional neural networks," *Pattern Recognit.*, vol. 77, pp. 248–261, May 2018.
[31] F. Costa, C. Levy, D. M. Xavier, M. Fujimoto, and F. Costa, "Automatic identification of tuberculosis mycobacterium," *Res.on Biomed. Eng.*, vol. 31, no. 1, pp. 33–43, 2015.
[32] K. Chakrabortya, A. Chattopadhyayb, A. Chakrabarti, T. Acharyad, and A. Dasguptae, "A combined algorithm for malaria detection from thick smear blood slides," *J. Health Med. Inf.*, vol. 6, no. 1, pp. 645–652, 2015.
[33] V. Makkapati, R. Agrawal, and R. Acharya, "Segmentation and classification of tuberculosis bacilli from zn-stained sputum smear images," in *Proc. CASE*, Aug. 2009, pp. 217–220.
[34] C. Li, K. Wang, and N. Xu, "A survey for the applications of content-based microscopic image analysis in microorganism classification domains," *Artif. Intell. Rev.*, vol. 51, no. 4, pp. 577–646, 2017.
[35] K. Simonyan and A. Zisserman, "Very deep convolutional networks for large-scale image recognition," 2014, *arXiv:1409.1556*. [Online]. Available: https://arxiv.org/abs/1409.1556
[36] V. Badrinarayanan, A. Handa, and R. Cipolla, "SegNet: A deep convolutional encoder-decoder architecture for robust semantic pixel-wise labelling," 2015, *arXiv:1505.07293*. [Online]. Available: https://arxiv.org/abs/1505.07293
[37] P. Kumar, P. Nagar, C. Arora, and A. Gupta, "U-segnet: Fully convolutional neural network based automated brain tissue segmentation tool," in *Proc. 25th IEEE Int. Conf. Image Process. (ICIP)*, Oct. 2018, pp. 3503–3507.
[38] K. Bhargavi and S. Jyothi, "A survey on threshold based segmentation technique in image processing," *Int. J. Innovative Res. Develop.*, vol. 3, no. 12, pp. 234–239, 2014.
[39] N. Senthilkumaran and R. Rajesh, "Edge detection techniques for image segmentation—A survey of soft computing approaches," *Int. J. Recent Trends Eng.*, vol. 1, no. 2, p. 250, 2009.
[40] Y. Xinmin, H. Beyenal, H. Gary, and L. Zbigniew, "Evaluation of biofilm image thresholding methods," *Water Res.*, vol. 35, no. 5, pp. 1149–1158, 2001.
[41] J. B. Xavier, A. Schnell, S. Wuertz, R. Palmer, D. C. White, and J. S. Almeida, "Objective threshold selection procedure (OTS) for segmentation of scanning laser confocal microscope images," *J. Microbiol. Methods*, vol. 47, no. 2, pp. 169–180, 2001.
[42] J. Kittler, J. Illingworth, and J. Föglein, "Threshold selection based on a simple image statistic," *Comput. Vis., Graph., image Process.*, vol. 30, no. 2, pp. 125–147, 1985.
[43] Y. Jerome, H. Yaoping, J. Steven, and M. Robert, "A two-step procedure for automatic and accurate segmentation of volumetric CLSM biofilm images," *J. Microbiol. Methods*, vol. 70, no. 3, pp. 424–433, 2007.
[44] M. G. Forero-Vargas, F. Sroubek, J. Alvarez-Borrego, N. Malpica, G. Cristobal, A. Santos, L. Alcala, M. Desco, and L. Cohen, "Segmentation, autofocusing and signagture extraction of tuberculosis sputum images," *Proc. SPIE*, vol. 4788, pp. 171–182, Nov. 2002.
[45] M. G. F. Costa, C. F. F. C. Filho, J. F. Sena, J. Salem, and M. O. de Lima, "Automatic identification of mycobacterium tuberculosis with conventional light microscopy," in *Proc. 30th Annu. Int. Conf. IEEE Eng. Med. Biol. Soc. (EMBS)*, Aug. 2008, pp. 382–385.
[46] R. Raof, Z. Salleh, S. I. Sahidan, M. Y. Mashor, S. S. M. Noor, F. M. Idris, and H. Hasan, "Color thresholding method for image segmentation algorithm of Ziehl-Neelsen sputum slide images," in *Proc. 5th Int. Conf. Elect. Eng., Comput. Sci. Autom. Control (CCE)*, 2008, pp. 212–217.
[47] N. Wahidah, N. Mustafa, M. Mashor, and S. Noor, "Comparison of color thresholding and global thresholding for Ziehl-Neelsen tb bacilli slide images in sputum samples," in *Proc. 2nd Int. Conf. Biomed. Eng. (ICoBE)*, 2015, pp. 1–6.
[48] R. Nikzad, P. Aleksandra, P. Wilfried, and O. Daniel, "Edge linking based method to detect and separate individual C. Elegans worms in culture," in *Proc. Digit. Image Comput., Techn. Appl. (DICTA)*, 2008, pp. 65–70.
[49] D. Rojas, L. Rueda, H. Urrutia, and A. Ngom, "Efficient optimal multilevel thresholding for biofilm image segmentation," in *Proc. Int. Conf. Pattern Recognit. Bioinformat. (IAPR)*, 2009, pp. 307–318.
[50] R. Dario and R. Luis, "Biofilm image segmentation using optimal multilevel thresholding," in *Proc. IEEE Int. Conf. Bioinformat. Biomed.*, Nov. 2009, pp. 185–190.
[51] R. Daro, R. Luis, N. Alioune, H. Homero, and C. Gerardo, "Image segmentation of biofilm structures using optimal multi-level thresholding," *Int. J. Data Mining Bioinformat.*, vol. 5, no. 3, pp. 266–286, 2011.
[52] H. P. and B. Parashuram, "Digital microscopic image analysis of spiral bacterial cell groups," in *Proc. Int. Conf. Intell. Syst. Data Process.*, 2011, pp. 209–213.
[53] K. Hak, K. Dong, J. Nam, S. Myung, and K. Lee, "Reconstruction and elimination of optical microscopic background using surface fitting method," *J. Fisheries Sci. Technol.*, vol. 1, no. 4, pp. 10–17, 2001.
[54] P. Rodrigues, A. H. J. Moreira, A. Teixeira-Castro, J. Oliveira, N. Dias, N. F. Rodrigues, and J. L. Vilaça, "Automatic segmentation and 3D feature extraction of protein aggregates in *caenorhabditis elegans*," *Proc. SPIE*, vol. 8317, p. 83170K, Apr. 2012.
[55] F. Levet, A. Cassany, M. Kann, and J.-B. Sibarita, "Automatic nonparametric capsid segmentation using wavelets transform and graph," in *Proc. 9th IEEE Int. Symp. Biomed. Imag. (ISBI)*, May 2012, pp. 1369–1372.
[56] H. B. Rachana and M. S. Swamy, "Automatic segmentation technique of tuberculosis bacilli in Ziehl-Neelsen-stained tissue images," in *Proc. Conf. Comput. Control Syst. Optim. (CCSO)*, 2013, pp. 5–7.
[57] Y. H. Wang, "Research on segmentation of protozoan and Metazoan image in microscopic examination of activated sludge," *Appl. Mech. Mater.*, vols. 448–453, pp. 367–370, Oct. 2014.
[58] P. Borges, B. Hamann, T. Silva, A. Vieira, and M. Oliveira, "A highly accurate level set approach for segmenting green microalgae images," in *Proc. 28th SIBGRAPI Conf. Graph., Patterns Images (SIBGRAPI)*, 2015, pp. 87–94.

[59] B. Khan, H. Nisar, C. Aun, and K. Lo, "Iterative region based Otsu thresholding of bright-field microscopic images of activated sludge," in *Proc. IEEE EMBS Conf. Biomed. Eng. Sci. (IECBES)*, Dec. 2016, pp. 533–538.

[60] S. E. V. Haryanto, M. Y. Mashor, A. S. A. Nasir, and H. Jaafar, "A fast and accurate detection of schizont plasmodium falciparum using channel color space segmentation method," in *Proc. 5th Int. Conf. Cyber IT Service Manage. (CITSM)*, 2017, pp. 1–4.

[61] K. Pho, T. Hirase, M. Amin, and A. Yoshitaka, "Protozoa identification using 3D geometric multiple color channel local feature," in *Proc. 10th Int. Conf. Knowl. Syst. Eng. (KSE)*, 2018, pp. 37–42.

[62] E. Battenberg and I. Bischofs-Pfeifer, "A system for automatic cell segmentation of bacterial microscopy images," Dept. Elect. Eng., Comput. Sci., Univ. California, Berkeley, Berkeley, CA, USA, Tech. Rep., 2006.

[63] P. Hiremath, P. Bannigidad, and M. Hiremath, "Automated identification and classification of rotavirus—A particles in digital microscopic images," in *Proc. Nat. Conf. Recent Trends Image Process. Pattern Recognit. (RTIPPR)*, 2010, pp. 69–73.

[64] F. Long, J. Zhou, and H. Peng, "Visualization and analysis of 3D microscopic images," *PLoS Comput. Biol.*, vol. 8, no. 6, p. e1002519, 2012.

[65] M. Chayadevi and G. Raju, "Automated colour segmentation of tuberculosis bacteria thru region growing: A novel approach," in *Proc. 5th Int. Conf. Appl. Digit. Inf. Web Technol. (ICADIWT)*, 2014, pp. 154–159.

[66] C. Xu, D. Zhou, T. Guan, and Y. Liu, "A segmentation algorithm for mycobacterium tuberculosis images based on automatic-marker watershed transform," in *Proc. IEEE Int. Conf. Robot. Biomimetics (ROBIO)*, Dec. 2014, pp. 94–98.

[67] R. Sznitman, A. Greenblum, P. Fua, P. Arratia, and J. Sznitman, "Caenorhabditis elegans segmentation using texture-based models for motility phenotyping," *IEEE Trans. Biomed. Eng.*, vol. 61, no. 8, pp. 2278–2289, Aug. 2014.

[68] X. Y. Lee, M. B. Khan, H. Nisar, Y. K. Ho, C. A. Ng, and A. S. Malik, "Morphological analysis of activated sludge flocs and filaments," in *Proc. IEEE Int. Instrum. Meas. Technol. Conf. (I2MTC)*, May 2014, pp. 1449–1453.

[69] E. Priya and S. Srinivasan, "Separation of overlapping bacilli in microscopic digital TB images," *Biocybern. Biomed. Eng.*, vol. 35, no. 2, pp. 87–99, 2015.

[70] M. I. Shah, S. Mishra, M. Sarkar, and S. K. Sudarshan, "Automatic detection and classification of tuberculosis bacilli from camera-enabled smartphone microscopic images," in *Proc. 4th Int. Conf. Parallel, Distrib. Grid Comput. (PDGC)*, 2016, pp. 287–290.

[71] M.-P. Dubuisson, A. K. Jain, and M. K. Jain, "Segmentation and classification of bacterial culture images," *J. Microbiol. Methods*, vol. 19, no. 4, pp. 279–285, 1994.

[72] M. E. Sieracki, S. E. Reichenbanch, and K. L. Webb, "Evaluation of automated threshold selection methods for accurately sizing microscopic fluorescent cells by image analysis," *Appl. Environ. Microbiol.*, vol. 55, no. 11, pp. 2762–2772, 1989.

[73] M. Forero, G. Cristobal, and J. Alvarez-Borrego, "Automatic identification techniques of tuberculosis bacteria," *Proc. SPIE*, vol. 5203, pp. 71–81, Nov. 2015.

[74] M. Daneshpanah and B. Javidi, "Segmentation of 3D holographic images using bivariate jointly distributed region snake," *Opt. Express*, vol. 14, no. 12, pp. 5143–5153, 2006.

[75] V. Pascal, M. Lisa, T. Lynne, and W. Cynthia, "Segmentation of dense 2D bacilli populations," in *Proc. Int. Conf. Digit. Image Comput., Techn. Appl.*, 2010, pp. 82–86.

[76] P. Hiremath, P. Bannigidad, and M. Hiremath, "Segmentation and identification of rotavirus—A in digital microscopic images using active contour model," in *Thinkquest~2010*. New Delhi, India: Springer, 2011, pp. 177–181.

[77] P. S. Hiremath and P. Bannigidad, "Spiral bacterial cell image analysis using active contour method," *Int. J. Comput. Appl.*, vol. 37, no. 8, pp. 5–9, 2012.

[78] E. Gutzeit, C. Scheel, T. Dolereit, and M. Rust, "Contour based split and merge segmentation and pre-classification of zooplankton in very large images," in *Proc. Int. Conf. Comput. Vis. Theory Appl. (VISAPP)*, vol. 1, 2014, pp. 417–424.

[79] M. Farahi, H. Rabbani, A. Talebi, O. Sarrafzadeh, and S. Ensafi, "Automatic segmentation of leishmania parasite in microscopic images using a modified cv level set method," in *Proc. 7th Int. Conf. Graphic Image Process. (ICGIP)*, vol. 9817, 2015, Art. no. 98170K.

[80] C. Li, K. Shirahama, and M. Grzegorzek, "Application of content-based image analysis to environmental microorganism classification," *Biocybern. Biomed. Eng.*, vol. 35, no. 1, pp. 10–21, 2015.

[81] C. Li and K. Shirahama, "Environmental microbiology aided by content-based image analysis," *Pattern Anal. Appl.*, vol. 19, no. 2, pp. 531–547, 2016.

[82] C. Li, K. Shirahama, J. Czajkowska, M. Grzegorzek, F. Ma, and B. Zhou, "A multi-stage approach for automatic classification of environmental microorganisms," in *Proc. Int. Conf. Image Process., Comput. Vis., Pattern Recognit. (IPCV)*, 2013, p. 1.

[83] C. Yang, C. Li, O. Tiebe, K. Shirahama, and M. Grzegorzek, "Shape-based classification of environmental microorganisms," in *Proc. 22nd Int. Conf. Pattern Recognit.*, 2014, pp. 3374–3379.

[84] Y. L. Zou, C. Li, Z. Boukhers, K. Shirahama, T. Jiang, and M. Grzegorzek, "Environmental microbiological content-based image retrieval system using internal structure histogram," in *Proc. 9th Int. Conf. Comput. Recognit. Syst. (CORES)*, 2016, pp. 543–552.

[85] Y. Zou, C. Li, K. Shirahama, T. Jiang, and M. Grzegorzek, "Content-based image retrieval of environmental microorganisms using double-stage optimisation-based fusion," in *Proc. Inf. Eng. Exp. Int. Inst. Appl. Informat.*, 2017, vol. 3, no. 4, pp. 43–53.

[86] F. Zhou and J. Liu, "Microbial contour extraction based on edge detection," in *Proc. 8th Int. Conf. Wireless Commun. Signal Process. (WCSP)*, 2016, pp. 1–5.

[87] H. Nisar, H. Y. Hang, S. C. Siang, and M. B. Khan, "Image segmentation of microscopic wastewater images using phase contrast microscopy," in *Proc. IEEE Conf. Syst., Process Control (ICSPC)*, Dec. 2016, pp. 102–106.

[88] M. B. Khan, H. Nisar, A. Ng, H. Yeap, and C. Lai, "Segmentation approach towards phase-contrast microscopic images of activated sludge to monitor the wastewater treatment," *Microscopy Microanal.*, vol. 23, no. 6, pp. 1130–1142, 2017.

[89] S. Iamsiri, N. Sanevas, C. Watcharopas, and P. Wattuya, "A new shape descriptor and segmentation algorithm for automated classifying of multiple-morphological filamentous algae," in *Proc. Int. Conf. Comput. Sci.*, 2019, pp. 149–163.

[90] S. Promdaen, P. Wattuya, and N. Sanevas, "Automated microalgae image classification," *Procedia Comput. Sci.*, vol. 29, pp. 1981–1992, Jan. 2014.

[91] M. K. Osman, M. Y. Mashor, and H. Jaafar, "Segmentation of tuberculosis bacilli in Ziehl-Neelsen tissue Sldie images using hibrid multilayered perceptron network," in *Proc. 10th Int. Conf. Inf. Sci., Signal Process. Appl. (ISSPA)*, 2010, pp. 365–368.

[92] P. Corina, A. Divekar, G. Coetzee, D. A. Clark, P. B. Fourie, F. Y. M. Lure, and S. Kennedy, "Application of stepwise binary decision classification for reduction of false positives in tuberculosis detection from smeared slides," in *Proc. Int. Conf. Image. Signal Process. Healthcare Technol.*, Washington, DC, USA, 2011, pp. 1–8.

[93] W. Maneesukasem and C. Pintavirooj, "Urine sediment image segmentation based on feedforward backpropagation neural network," in *Proc. Biomed. Eng. Int. Conf. (BMEiCON)*, Dec. 2012, pp. 1–4.

[94] R. Rulaningtyas, A. Suksmono, T. Mengko, and P. Saptawati, "Color segmentation using Bayesian method of tuberculosis bacteria images in Ziehl-Neelsen sputum smear," in *Proc. WiSE Health*, Surabaya, Indonesia, 2012.

[95] C. Suzuki, J. F. Gomes, A. X. Falcao, J. P. Papa, and S. Hoshino-Shimizu, "Automatic segmentation and classification of human intestinal parasites from microscopy images," *IEEE Trans. Biomed. Eng.*, vol. 60, no. 3, pp. 803–812, Mar. 2013.

[96] D. Nie, E. Shank, and V. Jojic, "A deep framework for bacterial image segmentation and classification," in *Proc. 6th ACM Conf. Bioinformat., Comput. Biol. Health Informat.*, 2015, pp. 306–314.

[97] V. Ayma, R. De Lamare, and B. Castañeda, "An adaptive filtering approach for segmentation of tuberculosis bacteria in Ziehl-Neelsen sputum stained images," in *Proc. Latin Amer. Congr. Comput. Intell. (LA-CCI)*, 2015, pp. 1–5.

[98] C. Li, K. Shirahama, and M. Grzegorzek, "Environmental microorganism classification using sparse coding and weakly supervised learning," in *Proc. 2nd Int. Workshop Environ. Multimedia Retr.*, 2015, pp. 9–14.

[99] K. Dannemiller, K. Ahmadi, and E. Salari, "A new method for the segmentation of algae images using retinex and support vector machine," in *Proc. IEEE Int. Conf. Electro/Inf. Technol. (EIT)*, Jun. 2015, pp. 361–364.

[100] S. Wiehman and H. de Villiers, "Semantic segmentation of bioimages using convolutional neural networks," in *Proc. Int. Joint Conf. Neural Netw. (IJCNN)*, 2016, pp. 624–631.

[101] X. Qiu, N. Tang, H. Zheng, G. Ji, and X. Qiao, "Automatic segmentation of chaetoceros microscopic images via pixel-wise classification," in *Proc. OCEANS-Shanghai*, 2016, pp. 1–5.

[102] J. Hung and A. Carpenter, "Applying faster R-CNN for object detection on malaria images," in *Proc. IEEE Conf. Comput. Vis. Pattern Recognit. Workshops*, Jul. 2017, pp. 56–61.
[103] A. Selman, A. Dubey, D. Dovrat, A. Aharoni, and R. Shilkrot, "CNN based yeast cell segmentation in multi-modal fluorescent microscopy data," in *Proc. IEEE Conf. Comput. Vis. Pattern Recognit. Workshops*, Jul. 2017, pp. 1–7.
[104] E. Ito, T. Sato, D. Sano, E. Utagawa, and T. Kato, "Virus particle detection by convolutional neural network in transmission electron microscopy images," *Food Environ. Virol.*, vol. 10, no. 2, pp. 201–208, 2018.
[105] M. Górriz, A. Aparicio, B. Raventós, V. Vilaplana, E. Sayrol, and D. López-Codina, "Leishmaniasis parasite segmentation and classification using deep learning," in *Proc. Int. Conf. Articulated Motion Deformable Objects*, 2018, pp. 53–62.
[106] A. Aziz, H. Pande, B. Cheluvaraju, and T. R. Dastidar, "Improved extraction of objects from urine microscopy images with unsupervised thresholding and supervised u-net techniques," in *Proc. IEEE Conf. Comput. Vis. Pattern Recognit. Workshops*, Jun. 2018, pp. 2230–2238.
[107] P. Andreini, S. Bonechi, M. Bianchini, A. Mecocci, and F. Scarselli, "A deep learning approach to bacterial colony segmentation," in *Proc. Int. Conf. Artif. Neural Netw.* Cham, Switzerland: Springer, 2018, pp. 522–533.
[108] R. B. Q. Ang, H. Nisar, M. B. Khan, and C.-Y. Tsai, "Image segmentation of activated sludge phase contrast images using phase stretch transform," *Microscopy*, vol. 68, no. 2, pp. 144–158, 2018.
[109] J. Matuszewski and I.-M. Sintorn, "Minimal annotation training for segmentation of microscopy images," in *Proc. IEEE 15th Int. Symp. Biomed. Imag. (ISBI)*, Apr. 2018, pp. 387–390.
[110] R. Chandan and D. Frank, "Computer-assisted segmentation of bacteria in color micrographs," *Microscopy Anal.*, vol. 18, no. 5, pp. 5–8, 2004.
[111] K. Matthew, G. Ling, and L. Steven, "Refining competition in the self-organising tree map for unsupervised biofilm image segmentation," *Neural Netw.*, vol. 18, nos. 5–6, pp. 850–860, 2005.
[112] C. Wählby, T. Riklin-Raviv, V. Ljosa, A. Conery, P. Golland, F. Ausubel, and A. E. Carpenter, "Resolving clustered worms via probabilistic shape models," in *Proc. IEEE Int. Symp. Biomed. Imag., From Nano Macro*, Apr. 2010, pp. 552–555.
[113] M. K. Osman, M. Y. Mashor, Z. Saad, and H. Jaafar, "Colour image segmentation of tuberculosis bacilli in Ziehl-Neelsen-stained tissue images using moving K-mean clustering procedure," in *Proc. 4th Asia Int. Conf. Math./Anal. Modeling Comput. Simulation (AMS)*, 2010, pp. 215–220.
[114] M. K. Osman, M. Y. Mashor, and H. Jaafar, "Detection of mycobacterium tuberculosis in Ziehl-Neelsen stained tissue images using Zernike moments and hybrid multilayered perceptron network," in *Proc. IEEE Int. Conf. Syst. Man (SMC)*, Oct. 2010, pp. 4049–4055.
[115] M. Ghosh, D. Das, C. Chakraborty, and A. Ray, "Plasmodium vivax segmentation using modified fuzzy divergence," in *Proc. Int. Conf. Image Inf. Process. (ICIIP)*, 2011, pp. 1–5.
[116] M. Osman, M. Mashor, and H. Jaafar, "Performance comparison of clustering and thresholding algorithms for tuberculosis bacilli segmentation," in *Proc. Int. Conf. Comput., Inf. Telecommun. Syst. (CITS)*, 2012, pp. 1–5.
[117] M. Kemmler, B. Fröhlich, E. Rodner, and J. Denzler, "Segmentation of microorganism in complex environments," *Pattern Recognit. Image Anal.*, vol. 23, no. 4, pp. 512–517, 2013.
[118] R. Rulaningtyas, B. Suksmono, T. Mengko, and P. Saptawati, "Multi patch approach in k-means clustering method for color image segmentation in pulmonary tuberculosis identification," in *Proc. 4th Int. Conf. Instrum., Commun., Inf. Technol., Biomed. Eng. (ICICI-BME)*, 2015, pp. 75–78.
[119] K. S. Mithra and W. R. S. Emmanuel, "Segmentation and classification of mycobacterium from Ziehl Neelsen stained sputum images for tuberculosis diagnosis," in *Proc. Int. Conf. Commun. Signal Process. (ICCSP)*, 2017, pp. 1672–1676.
[120] J. Wang, R. Sarkar, A. Aziz, A. Vaccari, A. Gahlmann, and S. T. Acton, "Bact-3D: A level set segmentation approach for dense multi-layered 3D bacterial biofilms," in *Proc. IEEE Int. Conf. Image Process. (ICIP)*, Sep. 2017, pp. 330–334.
[121] F. Hendrawan, V. Angkoso, and T. Wahyuningrum, "Colour image segmentation for malaria parasites detection using cascading method," in *Proc. Int. Conf. Sustain. Inf. Eng. Technol. (SIET)*, 2017, pp. 83–87.
[122] K. S. Mithra and W. R. S. Emmanuel, "An efficient approach to sputum image segmentation using improved fuzzy local information c means clustering algorithm for tuberculosis diagnosis," in *Proc. Int. Conf. Inventive Comput. Informat. (ICICI)*, 2017, pp. 126–130.
[123] M. Gadermayr, L. Gupta, B. M. Klinkhammer, P. Boor, and D. Merhof, "Unsupervisedly training GANs for segmenting digital pathology with automatically generated annotations," 2018, *arXiv:1805.10059*. [Online]. Available: https://arxiv.org/abs/1805.10059
[124] T. W. Ridler and S. Calvard, "Picture thresholding using an iterative selection method," *IEEE Trans. Syst., Man, Cybern.*, vol. SMC-8, no. 8, pp. 630–632, Aug. 1978.
[125] A. M. Khan and S. Ravi, "Image segmentation methods: A comparative study," *Int. J. Soft Comput. Eng.*, vol. 3, no. 4, pp. 84–92, 2013.
[126] S. Nagabhushana, *Computer Vision and Image Understanding*. New Delhi, India: New Age International, 2005.
[127] J. Ker, L. Wang, J. Rao, and T. Lim, "Deep learning applications in medical image analysis," *IEEE Access*, vol. 6, pp. 9375–9389, 2018.
[128] V. Chang, J. M. Saavedra, V. Castañeda, L. Sarabia, N. Hitschfeld, and S. Härtel, "Gold-standard and improved framework for sperm head segmentation," *Comput. Methods Programs Biomed.*, vol. 117, no. 2, pp. 225–237, 2014.
[129] P. Memmolo, G. Di Caprio, C. Distante, M. Paturzo, R. Puglisi, D. Balduzzi, A. Galli, G. Coppola, and P. Ferraro, "Identification of bovine sperm head for morphometry analysis in quantitative phase-contrast holographic microscopy," *Opt. Express*, vol. 19, no. 23, pp. 23215–23226, 2011.
[130] M. R. Ravanfar and M. H. Moradi, "Low contrast sperm detection and tracking by watershed algorithm and particle filter," in *Proc. 18th Iranian Conf. Biomed. Eng. (ICBME)*, 2011, pp. 260–263.
[131] Y. Ren, P. Wen, S. Li, Y. Liang, and W. Huang, "An improved algorithm of rat sperm image segmentation and counting," in *Proc. Int. Conf. Intell. Comput. Integr. Syst.*, 2010, pp. 201–204.
[132] P. S. Chandran, N. B. Byju, R. U. Deepak, R. R. Kumar, S. Sudhamony, P. Malm, and E. Bengtsson, "Cluster detection in cytology images using the cellgraph method," in *Proc. Int. Symp. Inf. Technol. Med. Educ. (ITME)*, vol. 2, Aug. 2012, pp. 923–927.
[133] F. Meyer, "Automatic screening of cytological specimens," *Comput. Vis., Graph., Image Process.*, vol. 35, no. 3, pp. 356–369, 1986.
[134] Y. M. George, H. H. Zayed, M. I. Roushdy, and B. M. Elbagoury, "Remote computer-aided breast cancer detection and diagnosis system based on cytological images," *IEEE Syst. J.*, vol. 8, no. 3, pp. 949–964, Sep. 2014.
[135] P. Wang, X. Hu, Y. Li, Q. Liu, and X. Zhu, "Automatic cell nuclei segmentation and classification of breast cancer histopathology images," *Signal Process.*, vol. 122, pp. 1–13, May 2016.
[136] N. Harandi, S. Sadri, N. Moghaddam, and R. Amirfattahi, "An automated method for segmentation of epithelial cervical cells in images of thin-prep," *J. Med. Syst.*, vol. 34, no. 6, pp. 1043–1058, 2010.
[137] Z. Lu, G. Carneiro, and A. P. Bradley, "Automated nucleus and cytoplasm segmentation of overlapping cervical cells," in *Proc. Int. Conf. Med. Image Comput. Comput.-Assist. Intervent*, 2013, pp. 452–460.
[138] G. Mehdi, V. Maheshwari, S. Afzal, H. Ansari, and I. Ahmad, "Image-guided fine-needle aspiration of retroperitoneal masses: The role of the cytopathologist," *J. Cytol./Indian Acad. Cytologists*, vol. 30, no. 1, p. 36, 2013.
[139] C. Jung and C. Kim, "Segmenting clustered nuclei using H-minima transform-based marker extraction and contour parameterization," *IEEE Trans. Biomed. Eng.*, vol. 57, no. 10, pp. 2600–2604, Oct. 2010.
[140] O. Sertel, U. Catalyurek, H. Shimada, and M. Gurcan, "Computer-aided prognosis of neuroblastoma: Detection of mitosis and karyorrhexis cells in digitized histological images," in *Proc. Annu. Int. Conf. IEEE Eng. Med. Biol. Soc.*, Sep. 2009, pp. 1433–1436.
[141] S. Di Cataldo, E. Ficarra, A. Acquaviva, and E. Macii, "Automated segmentation of tissue images for computerized IHC analysis," *Comput. Methods Programs Biomed.*, vol. 100, no. 1, pp. 1–15, 2010.
[142] J. Kong, L. Cooper, T. Kurc, D. Brat, and J. Saltz, "Towards building computerized image analysis framework for nucleus discrimination in microscopy images of diffuse glioma," in *Proc. Annu. Int. Conf. IEEE Eng. Med. Biol. Soc.*, Aug. 2011, pp. 6605–6608.
[143] N. Malpica, C. O. de Solórzano, J. J. Vaquero, A. Santos, I. Vallcorba, J. M. García-Sagredo, and F. del Pozo, "Applying watershed algorithms to the segmentation of clustered nuclei," *Cytometry*, vol. 28, no. 4, pp. 289–297, 1997.
[144] I. Goodfellow, J. Pouget-Abadie, B. Xu, D. Warde-Farley, S. Ozair, A. Courville, and Y. Bengio, "Generative adversarial nets," in *Proc. Adv. Neural Inf. Process. Syst.*, 2014, pp. 2672–2680.
[145] P. Luc, C. Couprie, S. Chintala, and J. Verbeek, "Semantic segmentation using adversarial networks," 2016, *arXiv:1611.08408*. [Online]. Available: https://arxiv.org/abs/1611.08408

[146] A. Radford, L. Metz, and S. Chintala, "Unsupervised representation learning with deep convolutional generative adversarial networks," 2015, *arXiv:1511.06434*. [Online]. Available: https://arxiv.org/abs/1511.06434
[147] D. Zhang, Y. Song, S. Liu, D. Feng, Y. Wang, and W. Cai, "Nuclei instance segmentation with dual contour-enhanced adversarial network," in *Proc. IEEE 15th Int. Symp. Biomed. Imag. (ISBI)*, Apr. 2018, pp. 409–412.
[148] Y. Zhang, L. Yang, J. Chen, M. Fredericksen, D. P. Hughes, and D. Z. Chen, "Deep adversarial networks for biomedical image segmentation utilizing unannotated images," in *Proc. Int. Conf. Med. Image Comput. Comput.-Assist. Intervent*, 2017, pp. 408–416.
[149] A. Arbelle and T. R. Raviv, "Microscopy cell segmentation via adversarial neural networks," in *Proc. IEEE 15th Int. Symp. Biomed. Imag. (ISBI)*, Apr. 2018, pp. 645–648.
[150] C. Li, *Content-based Microscopic Image Analysis*, vol. 39. Berlin, Germany: Logos Verlag, 2016.

FRANK KULWA was born in Tanzania, in 1986. He received the B.E. degree from the Dar es Salaam Institute of Technology, Tanzania, in 2013, where he has been a Tutorial Assistant, since 2017. Since 2018, he has been a master student with the Research Group for Microscopic Image and Medical Image Analysis, Northeastern University, China. His research interests include microorganism image analysis and deep learning.

CHEN LI received the B.E. degree from the University of Science and Technology Beijing, China, in 2008, the M.Sc. degree from Northeast Normal University, China, in 2011, and the Dr. Ing. degree from the University of Siegen, Germany, in 2016. From 2016 to 2017, he was a Postdoctoral Researcher with the Johannes Gutenberg University Mainz, Germany. He is currently an Associate Professor with Northeastern University, China, where he is the Head of the Research Group for Microscopic Image and Medical Image Analysis. His research interests include microscopic image analysis, medical image analysis, machine learning, pattern recognition, machine vision, multimedia retrieval, and membrane computing.

XIN ZHAO was born in 1982. He received the Ph.D. degree from the Harbin Institute of Technology, China, in 2011. He is currently an Associate Professor with the Environmental Engineering Institute, Northeastern University, China. He is also the Head of the Environmental Engineering Institute. His research interests include microbial molecular ecology and systems biology, water pollution control, and waste recycling.

BENCHENG CAI received the bachelor's degree from Sichuan University, China, in 2017. He is currently pursuing the master's degree with the Environmental Engineering Institute, Northeastern University, China. His research interests include microbial molecular ecology and systems biology.

NING XU received the bachelor's degree from Shenyang University, China, in 2008, the master's degree from Northeast Normal University, China, in 2011, and the Ph.D. degree from the University of Siegen, Germany, in 2016. Since 2017, she has been a Lecturer with the Liaoning Shihua University, China. Her research interests include image and video analysis.

SHOULIANG QI received the Ph.D. degree from Shanghai Jiaotong University, in 2007. He is currently an Associate Professor with Northeastern University, China. He joined the GE Global Research Center. From 2014 to 2015, he was a Visiting Scholar with the Eindhoven University of Technology and the Epilepsy Center Kempenhaeghe, The Netherlands. In recent years, he has been conducting productive studies in the intelligent medical imaging computing and modeling, machine learning, brain networks, and brain models. He has published over 80 papers in peer-reviewed journals and international conferences. He has received academic awards such as the Chinese Excellent Ph.D. Dissertation Nomination Award and the Award for Outstanding Achievement in Scientific Research from the Ministry of Education.

SHUO CHEN received the B.E. degree in biomedical engineering from Shanghai Jiaotong Univeristy, China, the M.S. degree in biomedical optics from Heidelberg University, Germany, and the Ph.D. degree in biomedical engineering from Nanyang Technological University, Singapore. He is currently an Associate Professor with Northeastern University, China. His research interests include biomedical optical spectroscopy and imaging, noninvasive medical diagnostics, biomedical instrumentation, and biomedical image processing.

YUEYANG TENG is currently an Associate Professor with the School of Medicine and Bioinformatics, Northeastern University, and the Young Director of the Artificial Intelligence Branch, Biomedical Engineering Society. From 2005 to 2013, he was with the PET-CT Research and Development Department of Shenyang Neusoft Medical System Company Ltd. Since 2013, he has been with Northeastern University, China. His research interests include machine learning (especially deep learning) theory and application, neuroinformatics, and biomedical imaging.